2008-07-15

A Comparative Analysis of Hydrolysis Kinetics by sPLA2 Isoforms During Apoptosis in S49 Cells

Erin Dalene Olson
Brigham Young University - Provo

A COMPARATIVE ANALYSIS OF HYDROLYSIS KINETICS BY $sPLA_2$ ISOFORMS DURING APOPTOSIS IN S49 CELLS

by

Erin D. Olson

A thesis submitted to the faculty of

Brigham Young University

In partial fulfillment of the requirements for the degree of

Master of Science

Department of Physiology & Developmental Biology

Brigham Young University

August 2008

BRIGHAM YOUNG UNIVERSITY

GRADUATE COMMITTEE APPROVAL

of a thesis submitted by

Erin D. Olson

This thesis has been read by each member of the following graduate committee and by majority vote has been found to be satisfactory.

_____	_____
Date	John D. Bell, Chair
_____	_____
Date	Allan M. Judd
_____	_____
Date	Allen R. Buskirk

BRIGHAM YOUNG UNIVERISTY

As chair of the candidate's graduate committee, I have read the thesis of Erin D. Olson in its final form and have found that (1) its format, citations, and bibliographical style are consistent and acceptable and fulfill university and department style requirements; (2) its illustrative materials including figures, tables, and charts are in place; (3) the final manuscript is satisfactory to the graduate committee and is ready for submission to the university library.

_____ _____

Date

John D. Bell
Chair, Graduate Committee

Accepted for the Department

_____

James P. Porter
Department Chair

Accepted for the College

_____

Rodney J. Brown
Dean, College of Life Sciences

ABSTRACT

A COMPARATIVE ANALYSIS OF HYDROLYSIS KINETICS BY $sPLA_2$ ISOFORMS DURING APOPTOSIS IN S49 CELLS

Erin D. Olson

Department of Physiology & Developmental Biology

Master of Science

Secretory Phospholipase A_2 ($sPLA_2$) represents a diverse class of roughly 20 enzymes, 12 of which have been identified in humans. These isoforms can be distinguished based on their tissue distribution, structure, and regulation. These differences in structure between the isoforms lead to the question does the enzyme's ability to respond to physical changes in the membrane during apoptosis governed by structure. S49 cell apoptosis was initiated by treatment with either the glucocorticoid dexamethasone (6–48 h) or with the calcium

ionophore, ionomycin. The rates of hydrolysis were compared with each treatment condition for various concentrations of snake venom and human groups (hG) IIA, V, and X isoforms. The data were analyzed using a model that explicitly evaluates both the adsorption of enzyme to the membrane surface (step 1) and subsequent binding of substrate to the active site (step 2). Increased hydrolysis during apoptosis appeared to reflect step 2 for both the snake venom and the hGX enzymes. In contrast, apoptosis promoted step 1 for hGV. For hGIIA, the kinetics were more complex suggesting additional mechanisms beyond these two steps. These observations are rationalized in terms of the structure of the various isozymes and physical changes during apoptosis, including reduction in the strength of lipid/neighbor interactions and increased bilayer surface charge.

ACKNOWLEDGEMENTS

I would first like to acknowledge the three mentors that that guided me through this study, namely; Dr. John Bell for all his patient tutorage and understanding throughout my studies in the biophysics great lab, as well as both Drs. Allan Judd and Allan Buskirk for their work on my committee. I also appreciate the work and camaraderie from my fellow graduate students, Rachel Bailey and Jennifer Keller. In addition, I would like to acknowledge the rest of the Bell lab for all of their support and participation in my thesis, especially Taylor Bruseke, Thao Nguyen, Elizabeth Gibbons, Aubrella Williamson, and Nick Gondala. Most importantly, I would like to acknowledge my husband, Eric Olson, for all his help and support.

This work was funded by NIH Grant GM073997, the BYU Cancer Research Center Graduate Summer Fellowship.

TABLE OF CONTENTS

LIST OF TABLES

LIST OF SCHEMES

LIST OF FIGURES

INTRODUCTION

There are two classical pathways in the cell death spectrum that are categorized as the extremes; apoptosis and necrosis. Necrosis is generally characterized by cells that have irreversible swelling of the cytoplasm and distortion of organelles. This mode of cell death usually occurs when cells have been exposed to hyperthermia, metabolic poisons and other direct traumas (1). Cells that undergo apoptosis can be biologically distinguished by their physical characteristics that include condensation of the cytoplasmic and nuclear membranes, microvesicle shedding, and blebbling of the plasma membrane. Biochemically, apoptosis is marked by DNA fragmentation, activation of aspartate-specific proteases known as caspases, and the exposure of phosphatidylserine (PS) on the outer leaflet of the membrane (2). Even though caspase activation is not necessary for apoptosis to occur, the morphological changes that characterize apoptosis are the direct result of caspase activation and cleavage (3, 4). Aside from the physical aspects, apoptosis also differs from necrosis by its functional role in development. The apoptosis pathway plays an integral role in cell proliferation, differentiation, activation, and removal during development. Because apoptosis is such an important component in the many stages of development, it can be considered as one of the fundamental aspects of cellular life (1, 2).

Within apoptosis, there are three phases; the initiation phase, the effector phase and the degradation phase. The initiation phase consists of cells receiving death-inducing signals that include the binding of certain ligands to death-transmitting receptors, and withholding of obligatory survival factors and

metabolite supply. After these signals are received, the effector phase is initiated and translates these signals into metabolic pathways, where the decision is finalized and the degradation phase is commenced (1).

Apoptosis occurs through either of two main (classical) pathways: the intrinsic pathway, which is a mitochondrial-dependent pathway, and the extrinsic/receptor-mediated pathway (2). The extrinsic pathway plays an integral role in inflammation and homeostasis of the tissue and can be activated through a variation of signaling cascades. Examples of these cascades include activation of a tumor necrosis factor family member, the Fas-Fas death receptor, or the localized secretion of lytic granules containing perforin on granzymes (2). An example of an apoptosis inducer that would use this pathway would be the ionophore, ionomycin (2, 5).

The intrinsic pathway is regulated by external cues and internal insults, such as proteins with death domains and DNA damage. In response to apoptotic stimuli given by the death domains, the outer mitochondrial membrane becomes permeable and releases cytochrome-c into the cytosol. Once released, cytochrome-c, interacts with Apoptotic protease-activating factor-1 (Apaf-1) which then activates a cascade of caspase proenzymes leading to apoptosis. An important regulator of this pathway, which contains both pro and anti-apoptotic members, is the Bcl-2 protein family (2). Both classical pathways then converge into a single pathway involving the activation of caspases that ultimately cleave regulatory and structural molecules, resulting in cell death.

However, recent studies have shown that there are exceptions employing a different route besides these two classical pathways. One exception is dexamethasone, a hormone that is part of a class of steroids called glucocorticoids (GC) (6). Instead of acting upon a death receptor or using mitochondrial response, these hormones bind to an intracellular glucocorticoid receptor (GR). After GC's pass through the membrane and dock onto the GR, the GR is released from its complex of heat shock proteins allowing it to pass through into the nucleus and bind to DNA or other transcription factors. Herald *et al.* state that even though GC-induced apoptosis does not proceed through one of the classic pathways, many genes or proteins such as caspases and Bcl-2 are activated and play crucial roles in this signaling cascade (6). Other examples of non-classical pathways include the Fas-ligand pathways used by cytotoxic T cells, or the perforin/granzyme B-dependent pathway used by natural killer cells (2).

Another event appearing to correspond with apoptosis, is the susceptibility of cells normally resistant to the enzyme secretory phospholipase A_2 ($sPLA_2$) (5, 7, 8). In addition to the ability of $sPLA_2$ to hydrolyze the sn-2 fatty acyl bond of membrane phospholipids, the enzyme is also able to differentiate between healthy and dying cells. This has been shown with the membranes of erythrocytes and S49 lymphoma cells (9, 10). However, the mechanism by which $sPLA_2$ distinguishes between healthy and apoptotic cells, after initial adsorption, is not yet known, but appears to involve changes in membrane physical properties (5). Nevertheless, these experiments have relied mostly on

$sPLA_2$ enzymes purified from various snake venoms, and not from enzymes found naturally within the human body. The relationship between apoptosis and susceptibility to human group isoforms has not yet been established.

Previously, a relationship has been shown between the structure of the various isoforms of $sPLA_2$ and their propensity for hydrolyzing artificial membranes possessing specific physical and chemical properties (11). One specific way in which these enzymes differ is their requirement for a negatively charged membrane to facilitate enzyme adsorption to the bilayer surface. For the hG-IIA enzyme, it is thought that a negative charge around the membrane is necessary for adsorption. In contrast, for the snake venom, hG-X, and the hG-V enzyme it is thought that a negatively charged membrane only enhances adsorption. Numerous studies have also demonstrated that membrane hydrolysis involves two steps (Scheme 1) (11, 12). The first step consists of enzyme adsorption to the phospholipid membrane, and the second step involves movement of the phospholipid head into the active site of the enzyme.

Based on these findings, we hypothesize that it is possible to say that the hG enzymes will behave the same when hydrolyzing nucleated cells as when they are interacting with artificial membranes. We also predict that (1) the afore mentioned model (Scheme 1) should hold true for the $sPLA_2$ isoforms, and (2) the differences between these isoforms would be in terms of the kinetic parameters, K_A and K_E, rather then in differences in the fundamental mechanics. These quantitative differences will distinguish the different isoforms of $sPLA_2$. However, the limiting step will continue to be the ability of the phospholipid to

access the active site of bound $sPLA_2$,and that this step will universally be a property of the membrane rather than of the enzyme. This hypothesis was tested by assessing the kinetics of membrane hydrolysis by four isoforms of $sPLA_2$ at various times during apoptosis and then comparing the results to enzyme structure and/or function. The $sPLA_2$ isoforms that were chosen were three recombinant human forms: (hG)—hG-IIA, hG-V, hG-X and snake venom from *Agkistrodon piscivorus piscivorus.* These variants were chosen because they have been well characterized structurally and enzymatically, and because they appear to have distinct functions within the human body. Human group IIA is synthesized in platelets and found in tears, and synovial fluid (13). Human group V is found primarily within the heart and is thought to be the evolutionary duplicate of the hG-IIA enzyme (14). Human group X is found mostly in immune tissues (13). Even though many questions have been answered about differences among these isoforms, results in current research are not yet sufficient to adequately compare hydrolysis kinetics in nucleated cells (14, 15).

The purpose of this study was to understand how apoptosis, induced by either a calcium ionophore or glucocorticoid, might increase the rate of phospholipid hydrolysis by extracellular $sPLA_2$. The basis for choosing ionomycin and dexamethasone as apoptotic reagents were for their similarities to natural causes of cell death. Ionomycin causes cell death by raising intracellular calcium to a high sustained level reminiscent of traumatic injury, or necrosis. In contrast, dexamethasone treatment emulates stress induced cortisol release and therefore emulates physiological induction of apoptosis. By further

understanding hydrolysis for both ends of the cell death spectrum (necrosis and apoptosis), we will be able to better characterize hydrolysis factors of the $sPLA_2$ enzyme and its isoforms.

Experiments for this study were designed to examine each of the parameters shown in Scheme 1 and to assess which step(s) is/are involved in distinguishing resistant cells from those treated with either ionomcyin or dexamethasone. The results demonstrate that among the different isoforms, modulation of either step one or step two (Scheme 1) may account for the increased susceptibility to $sPLA_2$, depending upon the isoform. In order to better visualize how Scheme 1 will be used to assess the limiting step for each isoform during hydrolysis, hypothetical graphs were created (Fig. 1). These graphs will be used as a standard in determining the limiting step.

MATERIALS AND METHODS

Reagents

The monomeric aspartate-49 phospholipase A_2 from the venom of *A. p. piscivorus* was isolated according to the procedure of Maraganore *et al.* (16). Recombinant hG-IIA and -X were provided by Michael Gelb and prepared using the procedures outlined in Baker and Markova *et.al*. respectively (14, 17). Human group V was provided by Wonwha Cho and was prepared according to Cho *et al.* (18). Ionomycin was purchased from Calbiochem (La Jolla, CA) and dissolved in dimethylsulfoxide (DMSO) for these experiments. Acrylodan-labeled

fatty acid-binding protein (ADIFAB), propidium iodide, cell culture medium, and serum were acquired from Invitrogen (Carlsbad, CA). Other reagents were obtained from standard sources. Probes were dissolved in various solvents as follows: ADIFAB in 50 mM KCl and 3 mM NaN_3, and propidium iodide in distilled water.

Cell Culture and Experimental Protocol

S49 mouse lymphoma cells were grown at 37 °C in humidified air, containing 10% CO_2, and prepared for experiments as described in Wilson *et al.* (19). Cell viability averaged 93 ± 3% (standard deviation) for control experiments, and ranged between 5 – 96% for treatment experiments. For spectral and kinetic experiments, an aliquot of cells (usually between 0.4–3.5 x 10^6 cells/ml in MBSS) was then transferred to a quartz fluorometer sample cell and allowed 5 min to equilibrate in the spectrofluorometer (Fluoromax 3, Horiba Jobin-Yvon, Edison, NJ). Spectral bandpass for experiments in the fluorometer were set at 4 nm. Data acquisition over time at multiple wavelengths (ADIFAB, propidium iodide) was accomplished by rapid sluing of fluorometer mirrors under the control of instrument software. Temperature and sample homogeneity were maintained as described previously in Harris *et al.* (20). All experiments and incubations were performed at 37 °C.

Membrane Hydrolysis

Ionomycin*:* The fluorescent fatty acid binding protein ADIFAB (excitation, 390 nm; emission, 432 nm and 505 nm) was used to assay the release of fatty acids from cell membranes in real time. After initiating data acquisition for 100 s, ADIFAB (65 nM final) and ionomycin (300 nM final) were added. At 700 s, a $sPLA_2$ isoform (0.7 – 70 nM final) was added and the time course continued for an additional 800-2000 s. Raw data were quantified by calculating the generalized polarization (GP) from the 432 and 505 intensities, and fitted to an arbitrary function by nonlinear regression (20).

Propidium iodide (PI) (37 μM final) (excitations at 537 and emission at 617) was used to assess how many cells had become permeable to the probe due to perturbations caused by hydrolysis as described in (19). Experimental protocol for PI was similar to that of ADIFAB, differing only in probe usage. Previous studies have demonstrated that assays with ADIFAB and propidium iodide provide identical results under conditions at which cells are susceptible to the enzyme's catalytic activity (19).

Dexamethasone: Experiments where cells that were treated with the glucocoritcoid, dexamethasone (100 nM final), for various lengths of time (6-48 hrs), or with varying concentrations at 24 h were the same. Hydrolysis and cell susceptibility were measured with ADIFAB and PI, respectively. After initiating data acquisition for 100 s, ADIFAB (65 nM final) and PI (37 μM final) were added. At 400 s, various isoforms (hG- IIA, -V, -X, and snake venom) of $sPLA_2$ (35 nM final for experiments were incubation length was varied, and 0.7 – 70 nM final for

experiments where enzyme concentrations was varied). At 1000 s ionomycin (300 nM final) was added and the time course continued for an additional 600–1000 s.

Propidium Iodide: Intensity of PI fluorescence was used to quantify cell susceptibility to the $sPLA_2$ enzyme, after control solvent (DMSO) or treatment (dexamethasone followed by ionomycin) was added to the samples. Data points between the time of PI addition and ionomycin addition were fit to an arbitrary function by nonlinear regression, and then were used to quantify the cells into different populations. These populations were then named for their distinct characteristics. Cells that took up PI immediately after addition of the probe were classified as “dead”; cells that took up PI only after addition of the enzyme isoform were classified as “alive but susceptible”; and cells that were only susceptible to the enzyme isoform after ionomycin addition were classified as “alive but resistant”. Data from the maximum fluorescence signal after ionomycin addition in control samples for each set of experiments were used as a standard to assess total cell hydrolysis. However, occasionally, the snake venom experimental sample was used as the standard when the control sample was unusable due to experimental complications. This standard was used to account for the cellular DNA that was completely fragmented during the experiment and was invisible to the probe. To account for variations of cell number, data were normalized to cell count (by hemocytometer and light microscopy) and light scatter values separately. For most experiments, an average of both light scatter

and cell count were used to improve accuracy. However, in some cases, only light scatter was used, due to erroneous cell counts.

Data Analysis: Data plotting, statistical tests and linear and nonlinear regression analyses were performed with Prism Graphpad software.

RESULTS

Ionomycin treatment was used to answer the following questions. First, what is the hydrolysis potency of each of the enzyme isoforms? Second, how do the human group isoform potencies compare to that of the snake venom isoform? Third, are the potencies for each of the isoforms significantly enhanced when treated with ionomycin compared to those of the control? Ionomcyin treatment was also used as a preliminary determinant for concluding which step in Scheme 1 is limiting for each of the isoforms.

Ionomcyin

Snake venom: Addition of $sPLA_2$ to S49 cells previously exposed (10 min) to a control vehicle (DMSO) caused a slight increase in ADIFAB GP followed by a gradual decline, nearly restoring the value to its original level (Fig. 2 curve b). Other studies show this unusual hydrolysis time course represents transient initial hydrolysis, followed by re-acylation of the lipids and reincorporation into the membrane. In contrast, prior exposure of cells to ionomycin resulted in a large

increase in ADIFAB GP that quickly reached a stable plateau (Fig. 2 curve a). ADIFAB is an acrylodan labled intestinal fatty acid binding protein. In the absence of fatty acid, the acrylodan fluorophore in ADIFAB occupies the free fatty acid binding site and fluoresces at 432 nm. In the presence of free floating fatty acids, the acrylodan fluorophore is displaced and exposed to the solvent and thus fluoresces at 505 nm. The sensitivity of acrylodan to the solvent relaxation effect results in a decrease of intensity at 432 nm that is directly proportional to the increase of intensity at 505 nm. This change in intensity is used to determine how much hydrolysis occurs during experiments.

In order to further characterize hydrolysis kinetics, the experiment represented in Figure 2 was repeated multiple times at various enzyme concentrations. Data were analyzed by nonlinear regression (examples are shown in Fig. 2). From these phenomenological fits, two parameters were determined: the initial rate of hydrolysis, and the maximum hydrolysis product generated. As displayed in Figure 3, treatment of cells with ionomycin increased both initial and total hydrolysis at all enzyme concentrations. The maximum hydrolysis rate was 0.018 ± 0.004 GP units s-1 for DMSO-treated samples and 0.093 ± 0.011 GP units s-1 for the ionomycin group. The enzyme concentration at which the hydrolysis rate was one-half the maximum, measured 13.5 ± 7.8 nM and 9.4 ± 3.2 nM for the two groups, respectively. Two-way analysis of variance indicated that both the effects of enzyme concentration and ionomycin treatment on the initial hydrolysis rate were highly significant ($p < 0.0001$). A significant interaction ($p < 0.0001$) between the two variables was also observed,

suggesting that the magnitude of the effect of ionomycin depended on enzyme concentration. The ability of ionomycin treatment to increase total hydrolysis product was also significant ($p < 0.0001$).

In addition to calculating the kinetic parameters in Figure 3 (V_{max} and EC_{50} values), we also compared the curves in Figure 3 to the hypothetical curves in Figure 1. This comparison illustrated the similarity between the snake venom isoform data in Figure 3, and the hypothetical curve for Scheme 1 where the limiting step is step two. These results suggest that the limiting step for the snake venom isoform is step two.

***Human group isoforms*:** S49 cells that were treated with the control vehicle (DMSO) showed no significant changes in ADIFAB GP upon addition of the hG-IIA and –V isoforms. Control experiments where cells were treated hG-X displayed a marginal increase of ADIFAB GP, followed by a gradual decline nearing the original values (Fig. 4: Panel D). The hG-X results were very similar to that of the snake venom ionomycin experiments, and it is thought that the same phenomenon of re-acylation is occurring. Exposure of the cells to ionomycin, showed an increase of both hydrolysis rate and amount for the hG-V and –X isoforms, and showed no effect on the rate or amount of hydrolysis for the hG-IIA isoform. Although, the extent of these increases depended upon the isoform and was always less than that observed with the snake venom enzyme

Of the three human group isoforms, hG-X was the most active upon cells treated with the calcium ionophore. Similar to that of the snake venom, the hG-X

isoform showed a large initial increase of hydrolysis that quickly reached a plateau (Fig. 4: Panel D). The hG-V isoform was the second most active, but enzyme activity was modest when compared to that of the hG-X or snake venom enzyme. Unlike that of the snake venom or the hG-X isoforms, hydrolysis by the hG-V isoform was gradual and never reached a plateau (Fig. 4: Panel C). Human group IIA hydrolyzed very little or no phospholipids from calcium ionophore-treated cells and showed no significant difference in ADIFAB GP between the control and treatment experiments (Fig. 4: Panel B).

Like in the snake venom section, we further characterized the hydrolysis kinetics of each $sPLA_2$ isoforms by calculating the initial rates. This was done by repeating the experiments of Figure 4 with varying concentrations of each isoform. The data were then analyzed using nonlinear regression (Fig. 5). As shown in Figure 5, there was an increase in initial hydrolysis rates for all isoforms except for hG-IIA (Fig. 5: Panel B), for which there was no consistent difference between ionomycin- and DMSO-treated samples. The maximum hydrolysis rates for each of the isoforms were calculated and are shown in Table 2. However, unlike the snake venom enzyme, there was no significant interaction between the two variables for the human group isoforms. We therefore conclude that ionomycin enhances hydrolysis for hG-V and –X isoforms, but not for the hG-IIA (Fig. 5).

Dexamethasone

The experiments with ionomycin were now expanded to include dexamethasone as the inducer of cell death. This was done for two reasons. First, we investigated how $sPLA_2$ isoforms differed in their hydrolysis abilities from one another in a physiological apoptotic setting. Second, we compared how hydrolysis differs in an apoptotic setting from that of a necrotic (ionomycin) setting.

Dexamethasone experiments were divided into two types of experiments; (1) experiments where incubation length varied while enzyme concentrations were held constant, and (2) experiments where incubation length was held constant while enzyme concentrations were varied. The first sets of experiments were used to determine when cells became susceptible to each of the isoforms and when maximum hydrolysis occurred, while the second set of experiments determined the maximum hydrolysis for each isoform.

Snake Venom: Addition of $sPLA_2$ to S49 cells incubated in a control vehicle (DMSO) for 24 h caused a slight increase in ADIFAB GP followed by a gradual decline, nearly restoring the value to its original level (Fig. 6: Panel A). Like in the ionomycin experiments, this unusual hydrolysis time course represents transient initial hydrolysis, followed by re-acylation of the lipids and reincorporation into the membrane (12). In contrast, 24 h incubation of cells in dexametheasone resulted in a large increase in ADIFAB GP that quickly reached a stable plateau (Fig. 6: Panel A). This sudden increase in ADIFAB GP is not

nearly as large as that of the ionomycin treatment; however, the increase is still significant.

Prolonged treatment with DMSO (up to 48 h) had no effect on the kinetics of membrane hydrolysis by $sPLA_2$ (data know shown). In contrast, cells exposed previously to dexamethasone for varying lengths of time (6-48 h) displayed an increase of substrate hydrolysis, as time progressed, reaching a state of maximum hydrolysis during 18-24 h of treatment. Hydrolysis then decreased at a moderate rate, to the point where hydrolysis was negligible (Fig. 7: Snake Venom row). The pooled values for the middle three time points (18,24,30 h) were distinguishable from zero by t-test (p= 0.0002); the pooled values for the early and late time points (9,40,48 h) were not significant (p= 0.0562).

In order to compare dexamethasone and ionomycin data, the initial rate and max hydrolysis of dexamethasone treatment was calculated. This was done through repeating experiments in Figure 6 with varying concentrations of enzyme (0.03–1.0 μg/ml). Data in Figure 8 showed an increase of hydrolysis as enzyme concentration increased (Fig. 8). Values for the maximum hydrolysis rate and the one-half the maximum were 0.2866 ± 0.01172 GP units s-1, and 0.1135 ± 0.01629 nM respectively. Like the ionomycin experiments, initial hydrolysis in dexamethasone-treated samples rapidly reached a plateau in lower levels of enzyme concentrations. Even though the amount of substrate hydrolyzed differs between the two treatments (ionomycin enhances greater), the EC_{50} values of ionomycin- and dexamethasone-treated cells are similar. Control treatment (DMSO) used for the dexamethasone experiments displayed no significant

increase of hydrolysis. The results in Figure 8, when compared to the hypothetical curves in Figure 1, are most similar to the curves in the panel where step two was limiting. These similarities to the ionomycin experiment and the step two hypothetical curves reinforce the suggestion that the limiting step for the snake venom enzyme is step two.

Varied Isoform concentrations with 24 h dexamethasone incubation for human group isoforms: As was observed with snake venom $sPLA_2$, incubation of cells with dexamethasone for 24 hrs enhanced the rate of hydrolysis, compared to control (DMSO) samples for each isoform (Fig. 6). However, the magnitude of the effect of dexamethasone differed among the isoforms, when compared to that obtained with ionomycin (Fig. 6). For example, hG-X behaved similar to the snake venom in that ionomycin was more effective at enhancing the rate of hydrolysis than was dexamethasone (Fig 6, Panels A and D). In contrast, the rate of hydrolysis catalyzed by either hG-IIA or hG-V was increased more by dexamethasone than by ionomycin (Panels B and C).

In order to compare dexamethasone and ionomycin data for each of the isoforms, the initial rate and max hydrolysis of dexamethasone treatment was calculated. This was done through repeating experiments in Figure 6 with varying concentrations of enzyme (0.03–1.0 μg/ml). The V_{max} and EC_{50} values for this analysis are shown in Table 2. Data from Figure 6 was also compared to the hypothetical curves from Scheme 1 in Figure 1. This comparison allowed us to preliminarily concluded that the limiting steps for the hG isoforms. They are as

follows: hG-X- step two; hG-V – step one; hG-IIA – inconclusive due to lack of response from ionomycin and DMSO treatments. These results also suggested that cells which undergo apoptosis are better hydrolyzed by the hGs-IIA and -V isoforms than cells that undergo necrosis.

Varied Dexamethasone incubation lengths with same enzyme concentration for human group isoforms: Cells that were incubated for various lengths of time (6-48hrs) with dexamethasone showed distinct similarities and differences in hydrolysis kinetics (Figs. 7, 9). Like the snake venom enzyme, all human group isoforms displayed enhanced hydrolysis for the first 24 h of dexamethasone incubation. Substrate hydrolysis for the hG-V and -X isoforms reach a maximum around 24 h dexamethasone treatment, while hG-IIA maximum hydrolysis is reached at around 18 h (Figs. 7, 9, and 10). This enhanced hydrolysis with the hG-IIA and -V isoforms only lasts for a short period time (4-6 hrs, or until after 24-25 h total incubation) before hydrolysis recedes back to zero (Figs. 7 and 9). Unlike the snake venome, hG-IIA, and -V isoforms, where hydrolysis returns to base level after prolonged dexamethasone treatment, hydrolysis by hG-X only slightly decreases (Fig. 9). A one sample t-test was performed on the dexamethasone data for each of the isoforms. For the hG-IIA and -V, the test demonstrated that hydrolysis for the middle time points were significantly different from zero (p = 0.0126, p = 0.0063), while the early and late time points were not significantly different (p = 0.0718, p =0.8692 respectively). Results for hG X enzyme showed a significant difference from zero for both sets

of time points (edge p = 0.0460, middle p = 0.0014). These delayed responses during apoptosis led us to conclude that there are certain apoptotic events that occur at these particular stages which increase the rate of hydrolysis.

Moreover, the data in Figure 9 also suggested that the identity of those events and/or their strength of coupling to hydrolysis might vary among the isoforms. To better understand the timing relationships among these isoforms, the number of cells categorized as “alive but susceptible” to hydorlysis by each isoform were compared. This number was assayed by the initial ability of cells to exclude propidium iodide, followed by uptake upon addition of enzyme as explained previously (Fig. 10) (7). This analysis, comparing the population of cells that are classified as “alive and susceptible” with extended dexamethasone incubations, showed a correlation between extended incubations and reduced cells susceptibility (Fig. 10). Figure 10 also displays that the peak activity time for each of the isoforms is still between 18-24 hrs.

To exclude time as a limiting factor for substrate hydrolysis, experiments for groups V and IIA were extended to 5000 seconds. Hydrolysis was then measured as mentioned above. Data illustrated that despite the time extension, maximum hydrolysis was still considerably less than that of the snake venom and hG-X isoforms (Data not shown).

DISCUSSION

Theoretical Analysis

Snake Venom: The model shown in Scheme 1 was used to analyze the results of the kinetic experiments displayed in Figs. 2 and 8. The initial rate of lipid catalysis (*dP/dt*) is given by

$$\frac{dP}{dt} = \frac{\beta K_A E_T K_E S_T}{1 + K_A E_T (1 + K_E S_T)}$$

eq 1

where β is proportional to *kcat* and the total number of adsorption sites for the enzyme (E_T) (9). It is assumed that β does not change with experimental treatment because alterations to membrane structure would presumably affect reaction steps preceding the catalytic event (9). For simplicity, β is assigned a value of 1.0 GP units s-1. S_T represents the mole fraction of membrane phospholipids available to the enzyme. In previous analyses, it has not been considered separately from K_E, since the two parameters are completely linked in the model (see Eq. 1) (9). However, the data of Fig. 3B demonstrate that S_T is subject to change upon experimental treatment and provide information to quantify the magnitude of that change. S_T is therefore included specifically as a parameter in Eq. 1 and expressed in relative units (*i.e.* it is assigned a value of 1.0 under control conditions).

As shown in Fig. 11A, the control data from Fig. 3A were well fit by Eq. 1. The value of K_A (6.7 × 107 M-1) matched favorably the value estimated from

competition with L-PLA2 (2.7 × 107 M-1 in reference iono paper). The effect of ionomycin on the initial hydrolysis rate was evaluated by considering S_T, K_A, and K_E individually in the fit, in order to identify the minimum criteria required by the results (parameter values summarized in Table 1). The data of Fig. 3B indicated that S_T increased by a factor of about 4.4 with ionophore treatment. Accordingly, Eq. 1 was re-calculated maintaining all parameter values from the fit of the control data with the exception of S_T. The 4.4-fold increase, however, was insufficient to account for the ionomycin data (Fig. 11B). In fact, a reasonable fit was obtained only with a much larger (8.1-fold) increase in S_T, one that cannot be justified based on the data of Fig. 3B (Fig. 11C). Since K_E and S_T are linked in Eq. 1, the dilemma can obviously be resolved by increasing K_E by a factor of 1.8 in addition to a fixed 4.4-fold increase in *ST* (Fig. 11D). Alternatively, allowing K_A to vary instead of K_E was inadequate to accommodate the data (Fig. 11E). The best fit, of course, was obtained when both K_A and K_E were allowed to float in combination with the prescribed increase in *ST* (Fig. 11F). This ideal fit corresponded to a 2-fold increase in K_E (in strong agreement with that of Panel D) coupled with a *reduction* in K_A by about 16% (corroborating the result in Panel E). Thus, we concluded from this analysis that increased susceptibility following ionomycin treatment has little or nothing to do with the strength of adsorption (K_A) and can be explained entirely by increases in the accessibility of lipids to the enzyme active site (K_E and S_T).

The intent of analyzing the two-step model, to the extant that was done with the ionomycin data, was to allow us to relate the information form the

arbitrary fits of the isoforms and dexamethasone treatment back to the model, with simple calculations. The model includes the calculation with equation 1 (21) and Figure 11 and Table 1. When the second step is a limiting step (and therefore enhanced by apoptosis), then the expected changes are seen in the max hydrolysis and not in the Kd for the enzyme. The converse is also true, when step one is the limiting step that is enhanced by apoptosis, where changes are expected to be seen between the Kd and not the max hydrolysis. These examples are illustrated by Figure 3 where the max hydrolysis rate was distinguishable and the half max was not distinguishable. By using this simple paradigm, step one and step two can be distinguished in the remaining of the isoforms, without the technical redundancy that is easily conveyed with one analysis.

In conclusion results from the ionomycin and dexamethasone experiments solidify the previous resolution that the limiting step in Scheme 1 for the snake venom enzyme is step two, or movement of the phospholipid head into the active site of the enzyme.

Isoforms: The fundamental objective to analyze the kinetic data in the context of Scheme 1 is to determine what elements of the catalytic mechanism are altered to produce increased hydrolysis during apoptosis. Specifically, the parameters assessed in the analysis, determine if cells permit hydrolysis to occur either because of increased adsorption (step one), or because of easier movement of phospholipids into the enzyme's active site (step two). Analysis results from the

ionomycin section contributed two important observations about the $sPLA_2$ enzyme. First, step one or step two can be distinguished as the limiting step if either V_{max} (step one) or EC_{50} (step two) changes. Second, the limiting step for snake venom is clearly step two, regardless whether apoptosis is initiated by ionomycin or dexamethasone.

Consequently, Scheme 1 was then used to asses the limiting step for each of the human group isoforms. Based on Figures 5 and 8 and the EC_{50} and V_{max} explanation above, values of K_A and K_E (Table 2) can be used to reveal which step is limiting within the reaction. To was done through calculating a global analysis of the data in Figure 8, in which each of the two fitting parameters (K_A/EC_{50} and K_E/V_{max}) were individually shared (and therefore held constant) among the data sets, or left to float (Fig. 12). For hG-X enzyme, data in Table 2 and in Figures 8 and 12 suggest that the limiting step in hydrolysis is step two. This was concluded by the similarity between the three EC_{50} values (ionomycin, dexamethasone and DMSO) that were calculated from nonlinear regression (Table 2), the similarity of those values to that of the EC_{50} values of the snake venom enzyme, and by the fact that the hG-X data in Figure 12 were best fit by varying V_{max}. Although, this was not the case with hG-V. When allowing the V_{max} to float while retaining EC_{50}, the global fits were unsatisfactory. However, by allowing EC_{50} to float while retaining V_{max}, the fits were greatly improved. This variance suggests the conclusion that enzyme adsorption, and not movement of the phospholipids into the active site, is the limiting step for the hG-V isoform.

This conclusion is supported by the fact that hG-V is noted for its affinity to anionic lipids, namely PS that are exposed during apoptosis (11).

Unlike the hG-X and V data in Figure 12 that clearly illustrates which step in Scheme 1 is limiting; results from nonlinear regression for the hG-IIA enzyme are unclear. However, because of the similarity between hG-IIA and hG-V (Fig. 8), we suggest that the limiting step may be step-one. This suggestion is reinforced by previous studies done by Sang *et al.* on anionic vesicles that conclude anionic vesicles increase binding affinity of the hG-IIA enzyme (11).

Negative Charge

It has been previously thought that PS exposure is the sole cause for increased enzyme binding affinity and hydrolysis for most isoforms (11). However, data presented in this thesis suggest that PS exposure may not be the only change in the membrane that increases hydrolysis. This assertion is based on results showing more anionic lipids are exposed in ionomycin-treated cells than in cells that have been treated with dexamethasone for 24 h (peak hydrolytic efficiency) (Figs. 4,6,8). This is because cells are simultaneously induced into apoptosis during ionomcyin treatments, and thus will have simultaneous PS exposure of about 100% (7). Whereas, with dexamethasone-treatment, cells do not progress simultaneously through apoptosis. Thus, PS flip-flop is less synchronized, and after 24 h, only averages about half the amount of that observed with ionomycin treatment (7). If PS exposure were indeed the only significant change in the membrane that enhances substrate hydrolysis, then the

results for all enzymes should have displayed more substrate hydrolyzed with ionomycin than with dexamethasone treatment at 24 h. However, since two enzymes (hG-IIA & hG-V) that are thought to be the most reliant on a negatively charged membrane (13) show no or very little hydrolysis when treated with ionomycin (Figs. 4, 5), we must conclude that there are other factors, in addition to PS exposure, that contribute to enhanced hydrolysis.

One of these factors could be oxidation of membrane phospholipids. This assumption is based on the studies of Fabisiak *et al.* and Salgo *et al*. who concluded that oxidized phospholipids provide a better substrate for $sPLA_2$ than negative phospholipids for most of the human group isoforms (22, 23). One of the main activators for phospholipid oxidation is the activation of cytochrome-c (23). It is also known that during the cascade of events in the dexamethasone pathway, cytochrome-c is turned on (6). By understanding these activation factors, the fact that dexamethasone-treated cells are hydrolyzed more efficiently by hG-IIA and –V is more easily understood.

Membrane Mechanics

Using a glucocorticoid, instead of an ionophore, provided a more comprehensive understanding of the mechanism by which the $sPLA_2$ enzyme increases hydrolysis in an *in vivo* environment, and a relative timetable of maximum cell susceptibility to the enzyme during apoptosis. Cells treated with dexamethasone and the snake venom enzyme displayed a greater increase in hydrolysis susceptibility at early stages of apoptosis than with the other isoforms.

Although the timing of structural changes in the membrane differs between the two pathways (10) (7), hydrolysis is still significantly increased for both ionomycin- and dexamethasone-treated cells (Figs. 4, 6, 8). This increased susceptibility illustrates the ability of the snake venom enzyme to hydrolyze cells with an amplified catalytic efficiency that is indifferent to the slight variations of membrane change that correspond with different apoptotic initiators and their relation to the cell death spectrum.

However, even with the increased catalytic efficiency shown in all isoforms of the $sPLA_2$ enzyme, the isoforms are still limited by membrane mechanics. As shown in Figures 7 and 9, the maximum amount of substrate hydrolysis for all isoforms occurs between 18-24 h incubation with dexamethasone. This significant increase in hydrolysis during this window of time correlates with data found in (10) demonstrating that during the same window, there is also an increase in lipid spacing and membrane hydration. Data in Figure 9 and 10 also illustrates that the snake venom, hG-IIA and –V enzymes hydrolyze significantly less substrate as the apoptosis process continues into later stages. This observation correlates with experiments showing that cell membranes progress into a more ordered state in the later stages of apoptosis (10). We therefore think this increase in order is one of the causes for decreased susceptibility as apoptosis progresses. This result refutes the previous assumption that dexamethasone-induced apoptosis enhances substrate hydrolysis by the $sPLA_2$ enzyme as incubation with the glucocorticoid is prolonged beyond 24h (7). However, this decrease in substrate hydrolysis does

not pertain to the hG-X enzyme (Fig. 9). The hG-X enzyme has the capacity to maintain the ability to hydrolyze substrate even while the membrane is highly ordered; leading us to the conclusion that membrane order is not a controlling factor in substrate availability.

While the majority of the activity of the enzymes decrease as order increases in the latter stages of apoptosis, it is unlikely that this latent resistance to $sPLA_2$ has any physiological significance since cells that are this far along in the apoptosis pathway would probably have been previously cleared by macrophages.

Structure and Function

hG-X: The ability of hG-X to hydrolyze highly ordered lipids while none of the other isoforms share this characteristic, suggested the exploration of the evolutionary development of the enzyme. According to Cupillard *et a*l. the hG-X enzyme is the ancestral human group $sPLA_2$ enzyme (24). This conclusion could explain why the hG-X is still in possession of this trait, and that the other variants of the $sPLA_2$ enzyme have lost the ability to hydrolyze highly ordered membranes, when specializing in specific functions.

There are several reasons why the hG-X isozyme behaves most similarly to the snake venom $sPLA_2$. One of these reasons stems from the fact that the hG-X isoform can hydrolyze both the zwitterionic and anionic phopholipid with similar catalytic efficiency (25). Pan *et al*. attribute this ability to the unique mixture of disulfide bonds found in the human group X enzyme (15). This

combination is a compilation of the disulfide bonds found in the structure of both the human groups I and II enzymes that could have a synergistic effect to increase hydrolysis (15).

A second reason that possibly accounts for the increased hydrolysis, is the ability of the enzyme to adsorb to the membrane (25). Ishimoto *et al*. state that the hG-X enzyme has a significantly increased rate of hydrolysis and binding to the phospholipid membrane, compared to hG-IIA and -V (25). Their data illustrate that the presence of phophatidylcholine increases hG-X hydrolysis of the membrane, by allowing the enzyme to initially adsorb better to the phospholipid membrane. Ishimoto *et al.* state that the reason for the increased adsorption of hG-X while in the presence of phosphatidylcholine is unknown. Nevertheless, they theorize that this phenomenon is physiological and suggest that hG-X has plays a role of relevance in the production of proatherogenic eicosanoids (25).

Pan *et al.* suggests a third reason that incorporates the structure of the enzyme and alternative physical attributes that contribute to hG-X ability to adsorb to and hydrolyze cellular membranes. According to Pan *et al*. (2002), one of the type-X characteristics that are thought to enhance hydrolysis includes a larger active site that accommodates the functional need to cleave phospholipids with the sn-2 polyunsaturated chain. Their study also noted that the hG-X isoform had a three-fold preference for phospholipids with an arachidonic acid side chain (15). These characteristics (an affinity for sn-2 fatty acids and interface site that is structured for larger phospholipid) show both the

evolutionary dexterity of the hG-X enzyme and the hydrolysis dexterity of the enzyme across the cell death spectrum.

hG-V/hG-IIA: Since the hG-V isoform is thought to be the evolutionary/functional duplicate of the hG-IIA (11), it is interesting to note the differences between the two enzymes. One of these differences is the effect of ionomycin on hydrolysis (Fig. 4). While hG-IIA seems to have no effect on cells that were treated with ionomycin, cells that were treated with the hG-V enzyme after ionomycin treatment showed an increased hydrolysis rate and amount as shown in Figures 4 and 5. This increase could be considered small when compared to either the hG-X or snake venom enzymes; however, it shows is a significant difference between the hG-IIA and the hG-V isoforms in their selectivity of membrane characteristics during apoptosis. One possible reason why hG-V has a higher catalytic activity than the hG-IIA enzyme is its ability to adsorb onto the membrane. It has been shown that a correlation between $sPLA_2$ isoforms that are in possession of tryptophans (or other aromatic side chains) on the interfacial binding surfaces and the enzyme's ability to hydrolyze cellular membranes (11). Han *et al*. then demonstrated that the higher binding affinity in the hG-V enzyme is attributed to the extra tryptophans that are situated on the putative interfacial binding surfaces.

In addition to the increased amount of tryptophans possessed by the hG-V isoform, we hypothesize there may be another, more physiological reason why substrate hydrolysis by hG-IIA is minimal in lymphoma cells when compared to

other isoforms. This concept incorporates the theory that the hG-IIA isoform has become specialized in its function. At some point in the evolutionary time scale, the hG-IIA isoform exchanged the ability to hydrolyze eukaryotic membranes at an increased catalytic rate, for the ability to hydrolyze bacterial membranes. Since bacteria are commonly found within and around the human body, this niche would be highly beneficial for the enzyme and its host.

CONCLUSION

There are four novel conclusions resulting from the data of this project. First, negative charge provided by exposed PS at the membrane surface is not the sole factor determining $sPLA_2$ adsorption/hydrolysis of the phospholipid membrane. Second, while snake venom, hG-IIA and hG-V isoforms do not hydrolyze highly ordered phospholipid membranes, the hG-X enzyme does. Third, all of the isoforms appear to benefit from changes that occur in the membrane during the early stages of apoptosis. Fourth, the limiting step in hydrolysis for each of the enzymes is as follows: snake venom- step two; hG-X- step two; hG-V- step one; and hG-IIA- inconclusive.

Reference List

1. Cohen, J. J., R. C. Duke, V. A. Fadok, and K. S. Sellins. 1992. Apoptosis and programmed cell death in immunity. *Annu. Rev. Immunol.* 10:267-293.
2. Fadeel, B. and S. Orrenius. 2005. Apoptosis: a basic biological phenomenon with wide-ranging implications in human disease. *J. Intern. Med.* 258:479-517.
3. Li, L. Y., X. Luo, and X. Wang. 2001. Endonuclease G is an apoptotic DNase when released from mitochondria. *Nature* 412:95-99.
4. Susin, S. A., H. K. Lorenzo, N. Zamzami, I. Marzo, B. E. Snow, G. M. Brothers, J. Mangion, E. Jacotot, P. Costantini, M. Loeffler, N. Larochette, D. R. Goodlett, R. Aebersold, D. P. Siderovski, J. M. Penninger, and G. Kroemer. 1999. Molecular characterization of mitochondrial apoptosis-inducing factor. *Nature* 397:441-446.
5. Kasibhatla, S., L. Genestier, and D. R. Green. 1999. Regulation of fas-ligand expression during activation-induced cell death in T lymphocytes via nuclear factor kappaB. *J. Biol. Chem.* 274:987-992.
6. Herold, M. J., K. G. McPherson, and H. M. Reichardt. 2006. Glucocorticoids in T cell apoptosis and function. *Cell Mol. Life Sci.* 63:60-72.
7. Nielson, K. H., C. A. Olsen, D. V. Allred, K. L. O'Neill, G. F. Burton, and J. D. Bell. 2000. Susceptibility of S49 lymphoma cell membranes to

hydrolysis by secretory phospholipase A(2) during early phase of apoptosis. *Biochim. Biophys. Acta* 1484:163-174.

8. Atsumi, G., M. Murakami, M. Tajima, S. Shimbara, N. Hara, and I. Kudo. 1997. The perturbed membrane of cells undergoing apoptosis is susceptible to type II secretory phospholipase A2 to liberate arachidonic acid. *Biochim. Biophys. Acta* 1349:43-54.
9. Jensen, L. B., N. K. Burgess, D. D. Gonda, E. Spencer, H. A. Wilson-Ashworth, E. Driscoll, M. P. Vu, J. L. Fairbourn, A. M. Judd, and J. D. Bell. 2005. Mechanisms governing the level of susceptibility of erythrocyte membranes to secretory phospholipase A2. *Biophys. J.* 88:2692-2705.
10. Bailey, R. W. 2008. Mechanisms by which apoptotic membranes become susceptible to secretory phospholipase A2. Brigham Young University.
11. Han, S. K., K. P. Kim, R. Koduri, L. Bittova, N. M. Munoz, A. R. Leff, D. C. Wilton, M. H. Gelb, and W. Cho. 1999. Roles of Trp31 in high membrane binding and proinflammatory activity of human group V phospholipase A2. *J. Biol. Chem.* 274:11881-11888.
12. Wilson, H. A., J. B. Waldrip, K. H. Nielson, A. M. Judd, S. K. Han, W. Cho, P. J. Sims, and J. D. Bell. 1999. Mechanisms by which elevated intracellular calcium induces S49 cell membranes to become susceptible to the action of secretory phospholipase A2. *J. Biol. Chem.* 274:11494-11504.

13. Koduri, R. S., J. O. Gronroos, V. J. Laine, C. Le Calvez, G. Lambeau, T. J. Nevalainen, and M. H. Gelb. 2002. Bactericidal properties of human and murine groups I, II, V, X, and XII secreted phospholipases A(2). *J. Biol. Chem.* 277:5849-5857.

14. Markova, M., R. A. Koratkar, K. A. Silverman, V. E. Sollars, M. MacPhee-Pellini, R. Walters, J. P. Palazzo, A. M. Buchberg, L. D. Siracusa, and S. A. Farber. 2005. Diversity in secreted PLA2-IIA activity among inbred mouse strains that are resistant or susceptible to Apc Min/+ tumorigenesis. *Oncogene* 24:6450-6458.

15. Pan, Y. H., B. Z. Yu, A. G. Singer, F. Ghomashchi, G. Lambeau, M. H. Gelb, M. K. Jain, and B. J. Bahnson. 2002. Crystal structure of human group X secreted phospholipase A2. Electrostatically neutral interfacial surface targets zwitterionic membranes. *J. Biol. Chem.* 277:29086-29093.

16. Maraganore, J. M., G. Merutka, W. Cho, W. Welches, F. J. Kezdy, and R. L. Heinrikson. 1984. A new class of phospholipases A2 with lysine in place of aspartate 49. Functional consequences for calcium and substrate binding. *J. Biol. Chem.* 259:13839-13843.

17. Baker, S. F., R. Othman, and D. C. Wilton. 1998. Tryptophan-containing mutant of human (group IIa) secreted phospholipase A2 has a dramatically increased ability to hydrolyze phosphatidylcholine vesicles and cell membranes. *Biochemistry* 37:13203-13211.

18. Cho, W., S. K. Han, B. I. Lee, Y. Snitko, and R. Dua. 1999. Purification and assay of mammalian group I and group IIa secretory phospholipase A2. *Methods Mol. Biol.* 109:31-38.

19. Wilson, H. A., W. Huang, J. B. Waldrip, A. M. Judd, L. P. Vernon, and J. D. Bell. 1997. Mechanisms by which thionin induces susceptibility of S49 cell membranes to extracellular phospholipase A2. *Biochim. Biophys. Acta* 1349:142-156.

20. Harris, F. M., S. K. Smith, and J. D. Bell. 2001. Physical properties of erythrocyte ghosts that determine susceptibility to secretory phospholipase A2. *J. Biol. Chem.* 276:22722-22731.

21. Bailey, R. W., E. D. Olson, M. P. Vu, T. J. Brueseke, L. Robertson, R. E. Christensen, K. H. Parker, A. M. Judd, and J. D. Bell. 2007. Relationship between Membrane Physical Properties and Secretory Phospholipase A2 Hydrolysis Kinetics in S49 Cells during Ionophore-Induced Apoptosis. *Biophys. J.* 93:2350-2362.

22. Salgo, M. G., F. P. Corongiu, and A. Sevanian. 1993. Enhanced interfacial catalysis and hydrolytic specificity of phospholipase A2 toward peroxidized phosphatidylcholine vesicles. *Arch. Biochem. Biophys.* 304:123-132.

23. Fabisiak, J. P., V. E. Kagan, Y. Y. Tyurina, V. A. Tyurin, and J. S. Lazo. 1998. Paraquat-induced phosphatidylserine oxidation and apoptosis are independent of activation of PLA2. *Am. J. Physiol* 274:L793-L802.

24. Cupillard, L., K. Koumanov, M. G. Mattei, M. Lazdunski, and G. Lambeau. 1997. Cloning, chromosomal mapping, and expression of a novel human secretory phospholipase A2. *J. Biol. Chem.* 272:15745-15752.

25. Ishimoto, Y., K. Yamada, S. Yamamoto, T. Ono, M. Notoya, and K. Hanasaki. 2003. Group V and X secretory phospholipase A(2)s-induced modification of high-density lipoprotein linked to the reduction of its antiatherogenic functions. *Biochim. Biophys. Acta* 1642:129-138.

SCHEME 1 Reaction scheme for interaction between $sPLA_2$ and cell membranes. *E*, free $sPLA_2$; *EB*, $sPLA_2$ adsorbed to membrane surface sites (*Ms*); *S*, available substrate (membrane phospholipid); *EB s*, adsorbed enzyme with substrate bound to the active site; K_A, equilibrium constant for enzyme adsorption to the membrane; K_E, equilibrium constant for substrate migration into the enzyme active site; *kcat*, turnover number for substrate hydrolysis; *P*, product (fatty acid).

FIGURE 1: Hypothetical curves for the analysis of Scheme 1. Panel A displays if adsorption, step-one, was the limiting step. EC_{50} was left to float while V_{max} was held constant. Panel B displays if the phospholipids movement into the active site, step-two, is the limiting step. V_{max} was allowed to float while EC_{50} was held constant. In each panel the red curve represents ionomycin/ dexamethasone treatment and the blue curve represents the control/DMSO treatment.

FIGURE 2: Effects of ionomycin treatment on the time course of membrane hydrolysis by $sPLA_2$. S49 cells were incubated with ADIFAB and treated for at least 600 s with DMSO (curve a) or ionomycin (curve b) as explained in Materials and Methods. At the time indicated by the *arrows*, $sPLA_2$ (70 nM final) was added. Data points represent the raw data (expressed in GP units), and curves represent nonlinear regression fits of the data using an arbitrary function consisting of the sum of two exponential functions. The amount of hydrolysis observed in curve b constitutes approximately 2–5% of the plasma membrane phospholipid (1).

FIGURE 3: Secretory PLA_2 concentration dependence of the initial rate of hydrolysis. Panel A: the experiments of Fig. 1 were repeated at the indicated concentrations of $sPLA_2$ for cells treated with DMSO (squares) or ionomycin (triangles). The initial rate was defined as the amount of product generated during 5 s from the time of enzyme addition. This number was calculated from nonlinear regression fits of the data as shown in Fig. 1. Data were analyzed by two-way analysis of variance to assess the contribution of $sPLA_2$ concentration (37% of variation, $p < 0.0001$), ionomycin treatment (13% of variation, $p < 0.0001$), and the interaction between the two (20% of variation, $p < 0.0001$). Data points represent the raw data (expressed in GP units), and curves represent nonlinear regression fits of the data using an arbitrary function. Panel B: the total amount of product after 600 s (or at the maximum for time courses shaped like that of curve a in Fig. 1) for enzyme concentrations ≥18 nM. The data were significant based on two-tailed unpaired Student's t test ($p < 0.0001$, n = 1–4 at each datum).

FIGURE 4: Ionomycin treatment has varying effects on $sPLA_2$ isoforms. S49 cells were incubated with ADIFAB and treated for at least 700 s with DMSO (blue curve) or ionomycin (red curve) as explained in Materials and Methods. At around 700 s, $sPLA_2$ (35 nM final) was added. Panel A: addition of snake venom

enzyme; Panel B: addition off hG-IIA enzyme; Panel C: addition of hG-V enzyme; Panel D: addition of hG-X enzyme. Curves are raw data represented by ADIFAB GP.

FIGURE 5: Ionomycin treatment increases the amount and initial rate of membrane hydrolysis by $sPLA_2$: Experiments of Figure 4 were repeated at the indicated concentrations of $sPLA_2$ isoforms for cells treated with DMSO (squares) or ionomycin (circles). The initial rate was defined as the amount of product generated during time indicated in panel from the time of enzyme addition. Initial rates were calculated at 10s for snake venom, 300s for hG IIA, and 100s for hG V and hG X. This number was calculated from nonlinear regression fits of the data as shown in Figures 1 and 4 (data not shown).

FIGURE 6: Dexamethasone causes increased activity for all isoforms. Cells were treated with dexamethasone (black) or DMSO (blue) for 24 h prior to enzyme addition (~750 s). At around 700 s, $sPLA_2$ (35 nM final) was added. Panel A: addition of snake venom enzyme; Panel B: addition off hG-IIA enzyme; Panel C: addition of hG-V enzyme; Panel D: addition of hG-X enzyme. Curves are raw data represented by ADIFAB GP.

FIGURE 7: Effect of dexamethasone incubation time on membrane hydrolysis by $sPLA_2$ isoforms. S49 cells were incubated with dexamethasone for varying lengths of time (6-48 hrs). At 100 s samples were treated with ADIFAB and left to incubate for 600 s as explained in Materials and Methods. At the time 750 s $sPLA_2$ (70 nM final) was added. Curves are raw data represented by ADIFAB GP.

FIGURE 8: Dexamethasone treatment increases initial hydrolysis by all isoforms: Experiments of Figure 6 were repeated at the indicated concentrations of $sPLA_2$ isoforms for cells treated with DMSO (squares),ionomycin (triangles), or dexamethasone (circle). The initial rate was defined as the amount of product generated during time indicated in panel from the time of enzyme addition. Initial rates were calculated at 10s for snake venom, 300s for hG IIA, and 100s for hG V and hG X. This number was calculated from nonlinear regression fits of the data as shown in Figures 3 and 5. Ionomycin and DMSO data taken from Figure 6. Nonlinear regression fits of the data calculated the apparent dissociation constants represented in the table below.

FIGURE 9: Summary of hydrolysis experiments by $sPLA_2$ isoforms. A comparison of hydrolysis by $sPLA_2$ isoforms when cells are treated with dexamethasone. One sample t-test was performed on each of the isoforms, dividing the data into two groups. Group a consisting of the outside, or early and late, time points, and group b consisted of the middle three time points. For the snake venom, hG IIA and V there was a significant difference between the middle time points and zero but not the outside time points. For the hG-X enzyme both sets of data points were significantly different from zero.

FIGURE 10: Percent of cells that are categorized as Alive and Susceptible from propidium Iodide data graphed against time. S49 cells that have been treated with dexamethasone for varying lengths of time (6-48 h) show a decrease in cells that are susceptible to the enzyme as incubation time increases. Data points represent the average of cells that are categorized as cells that are alive and susceptible, and the error bars represent the standard error of the mean.

FIGURE 11: Analysis of hydrolysis results in terms of Scheme 1. Initial $sPLA_2$ hydrolysis rates from Fig. 2A were fit by nonlinear regression to Eq. 1 multiple times with various combinations of constraints. Panel A: baseline parameter values were obtained by fitting the control (DMSO) data from Fig. 2A; parameter values are listed in the first row of Table 1. Some parameters were allowed to float in fits of the ionomycin data (Panels B–F) as detailed below. S_T was fixed at 1.0 GP units in Panel A and at 4.66 GP units with the ionomycin data (except in Panel C) as explained in the text. The remaining parameters were kept fixed at the values obtained in Panel A (details in rows 2–6 of Table 1). The parameters allowed to float during the fits for each panel were: Panel B: none, Panel C: S_T, Panel D: K_E, Panel E: K_A, Panel F: K_E and K_A.

FIGURE 12: Analysis of hydrolysis results in terms of Scheme 1 for $sPLA_2$ isoforms. Initial $sPLA_2$ hydrolysis rates from Fig. 8 Panels C (hGV) and D (hG X) were fit by nonlinear regression to Eq. 1 multiple times with various combinations of constraints. Some parameters were allowed to float in fits of the ionomycin, DMSO and dexamethasone data (Black = dex, Blue = DMSO, Red = ionomcyin) as detailed below. Panel A: baseline parameter values were obtained by fitting the control (DMSO) data from Fig. 8C (Blue solid, doted and dashed lines). The parameters allowed to float during the fits for each treatment were: Dashed line: none, Solid line: K_E (shared max), Dotted line: K_A (Shared Kd).

TABLE 1 Parameter values for Fig. 11.

	Parameters			
Fig. 11 Panel	β (GP units s^{-1})	K_A (nM^{-1})	K_E	S_T (relative
A	1.0	0.067	0.10	1.0
B	1.0	0.067	0.10	4.43
C	1.0	0.067	0.10	8.12
D	1.0	0.067	0.18	4.43
E	1.0	0.273	0.10	4.43
F	1.0	0.056	0.20	4.43

Parameter values were obtained by nonlinear regression using Eq. 2 as explained in the legend to Fig. 11. Values allowed to float in the regression are underscored

.

TABLE 2 Parameter values for Fig. 8

Table 3

Treatment	Parameters	hG-IIA	hG-V	hG-X
Dex	EC_{50} nM^{-1}	2.7 ± 1.5	0.22 ± 0.08	0.15 ± 0.02
Dex	V_{max} GP units s^{-}	0.62 ± 0.23	0.24 ± 0.03	0.52 ± 0.02
Ionomyci	EC_{50} nM^{-1}	N/A	1.10 ± 0.97	0.12 ± 0.07
Ionomyci	V_{max} GP units s^{-}	N/A	0.28 ± 0.15	0.67 ± 0.12
DMSO	EC_{50} nM^{-1}	N/A	1.3 ± 1.2	0.39 ± 0.54
DMSO	V_{max} GP units s^{-}	N/A	0.18 ± 0.10	0.31 ± 0.17

Parameter values were obtained by nonlinear regression using Eq. 1 as explained in the legend to Fig. 8.

SCHEME 1

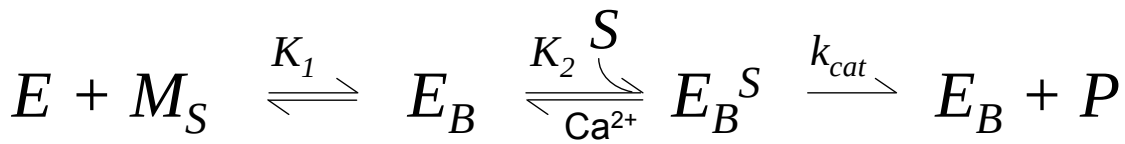

FIGURE 1

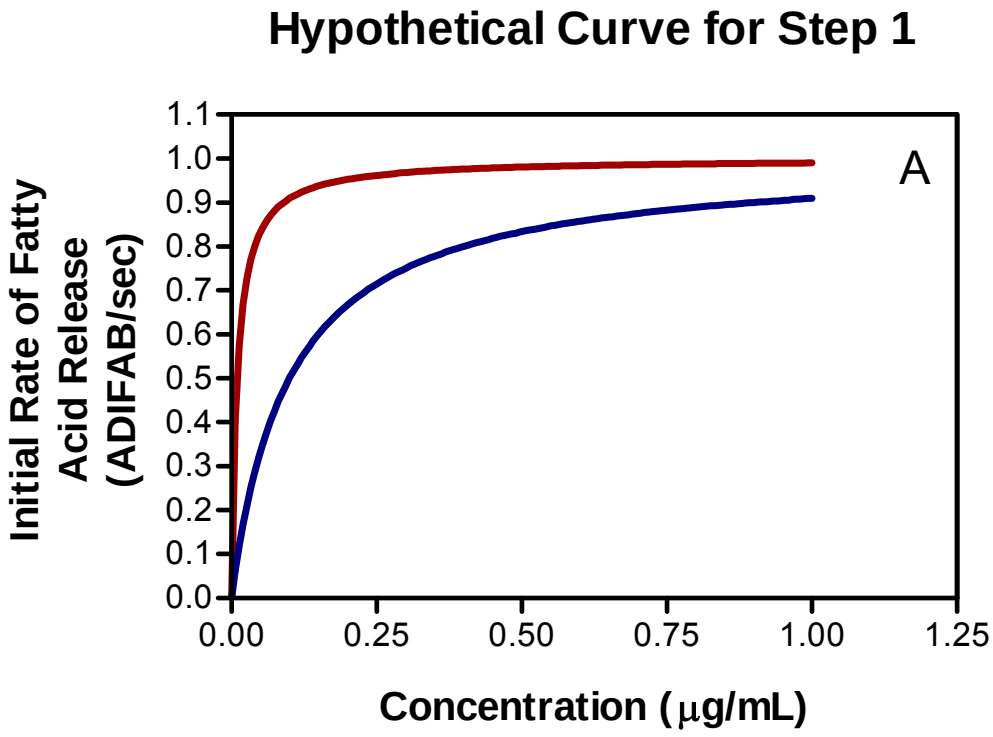
Hypothetical Curve for Step 1
Initial Rate of Fatty Acid Release (ADIFAB/sec)
1.1
1.0
0.9
0.8
0.7
0.6
0.5
0.4
0.3
0.2
0.1
0.0
A
0.00
0.25
0.50
0.75
1.00
1.25
Concentration (μg/mL)

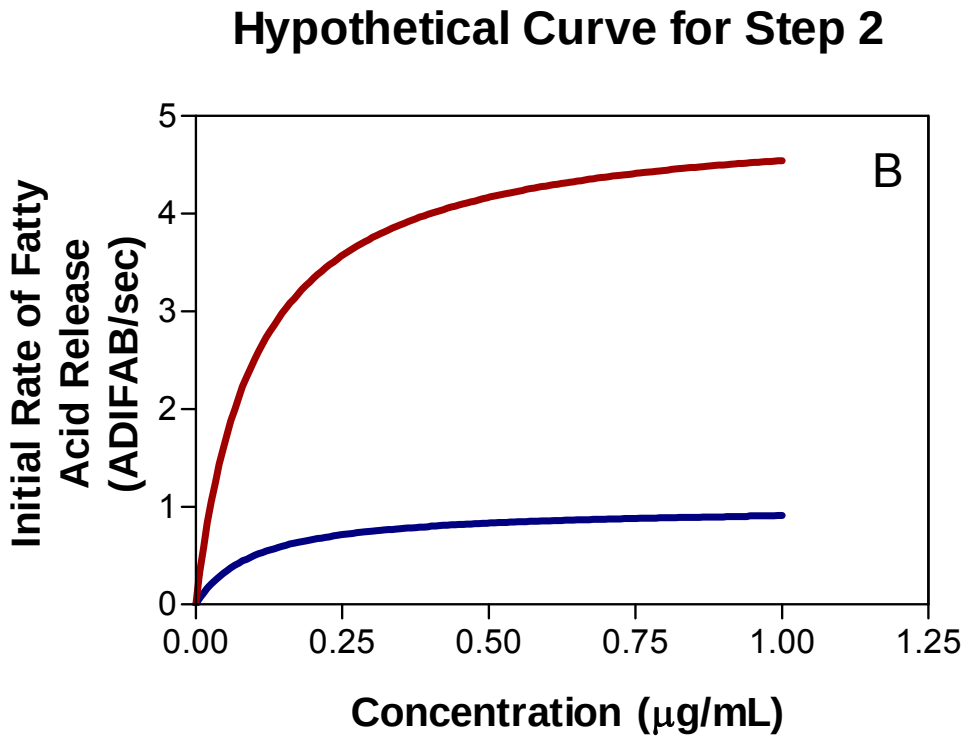
Hypothetical Curve for Step 2
Initial Rate of Fatty Acid Release (ADIFAB/sec)
5
4
3
2
1
0
B
0.00
0.25
0.50
0.75
1.00
1.25
Concentration (μg/mL)

FIGURE 2

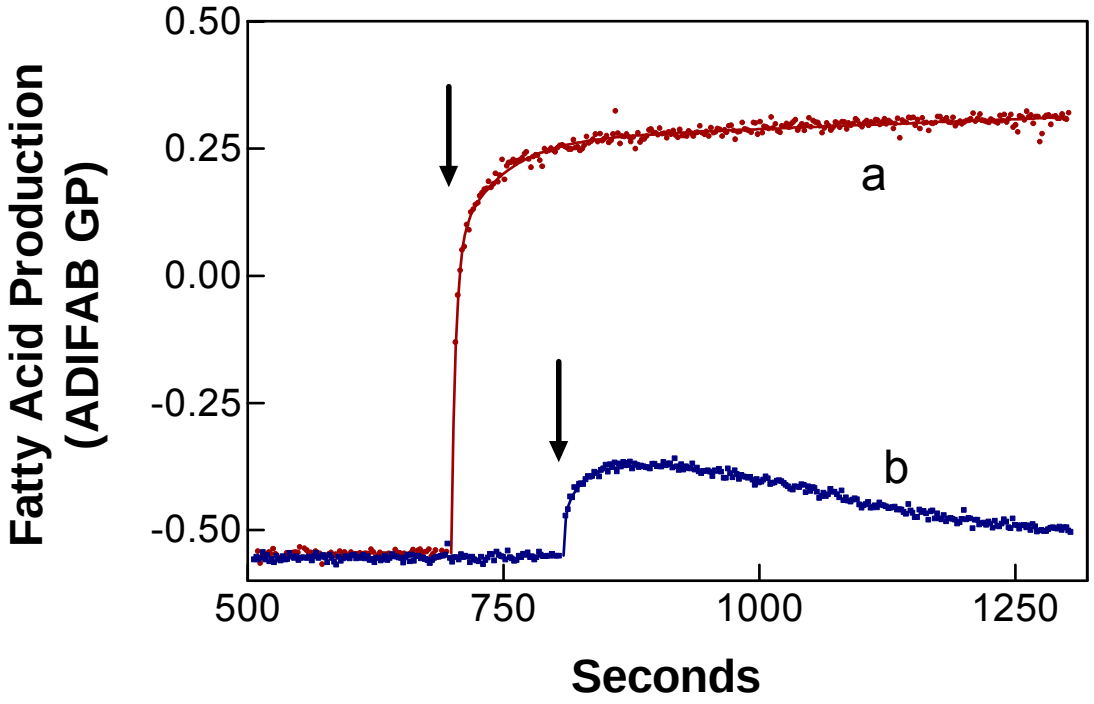
Fatty Acid Production
(ADIFAB GP)
0.50
0.25
0.00
-0.25
-0.50
500
750
1000
1250
Seconds
a
b

FIGURE 3

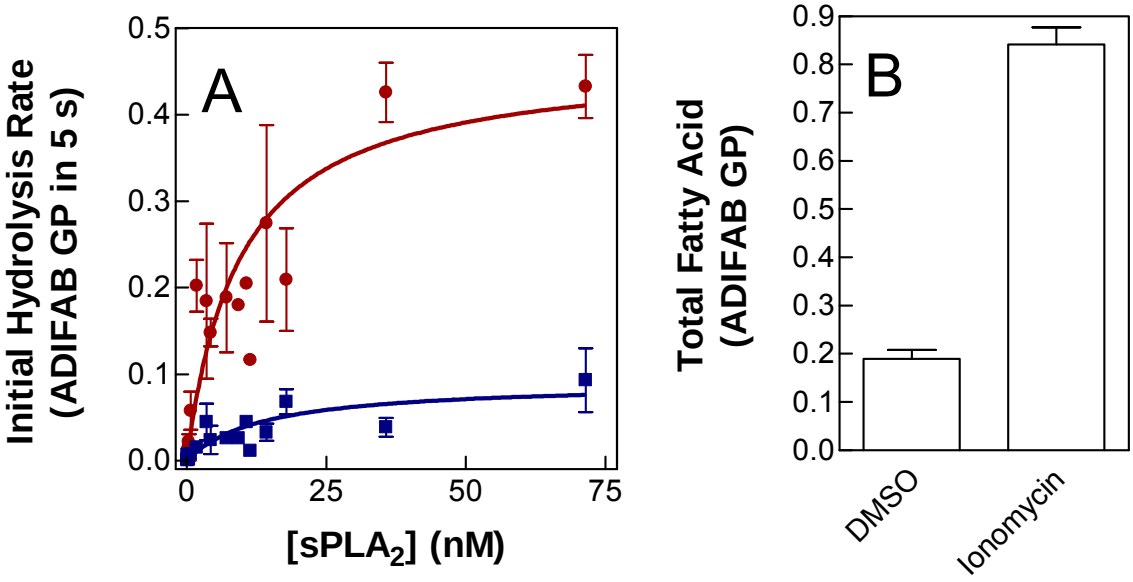
A
Initial Hydrolysis Rate
(ADIFAB GP in 5 s)
0.5
0.4
0.3
0.2
0.1
0.0
0
25
50
75
[sPLA2] (nM)
B
Total Fatty Acid
(ADIFAB GP)
0.9
0.8
0.7
0.6
0.5
0.4
0.3
0.2
0.1
0.0
DMSO
Ionomycin

FIGURE 4

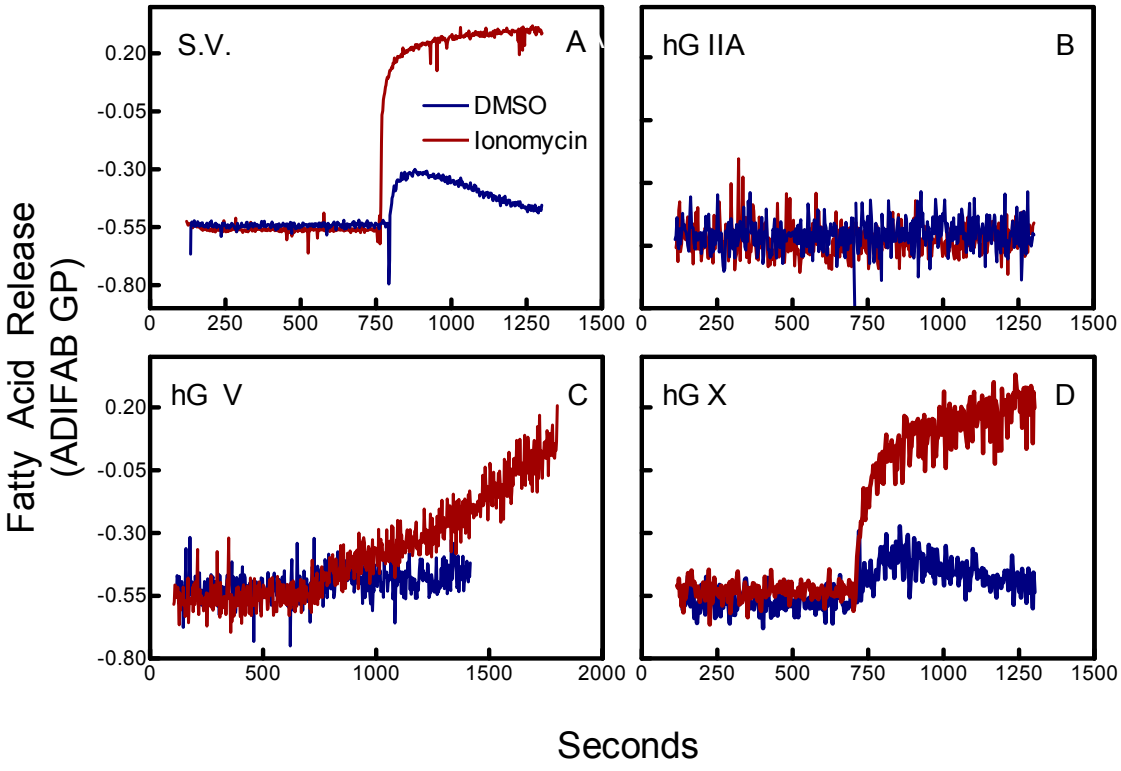
S.V.
A
DMSO
Ionomycin
hG IIA
B
hG V
C
hG X
D
Fatty Acid Release
(ADIFAB GP)
Seconds
0.20
-0.05
-0.30
-0.55
-0.80
0
250
500
750
1000
1250
1500
2000

FIGURE 5

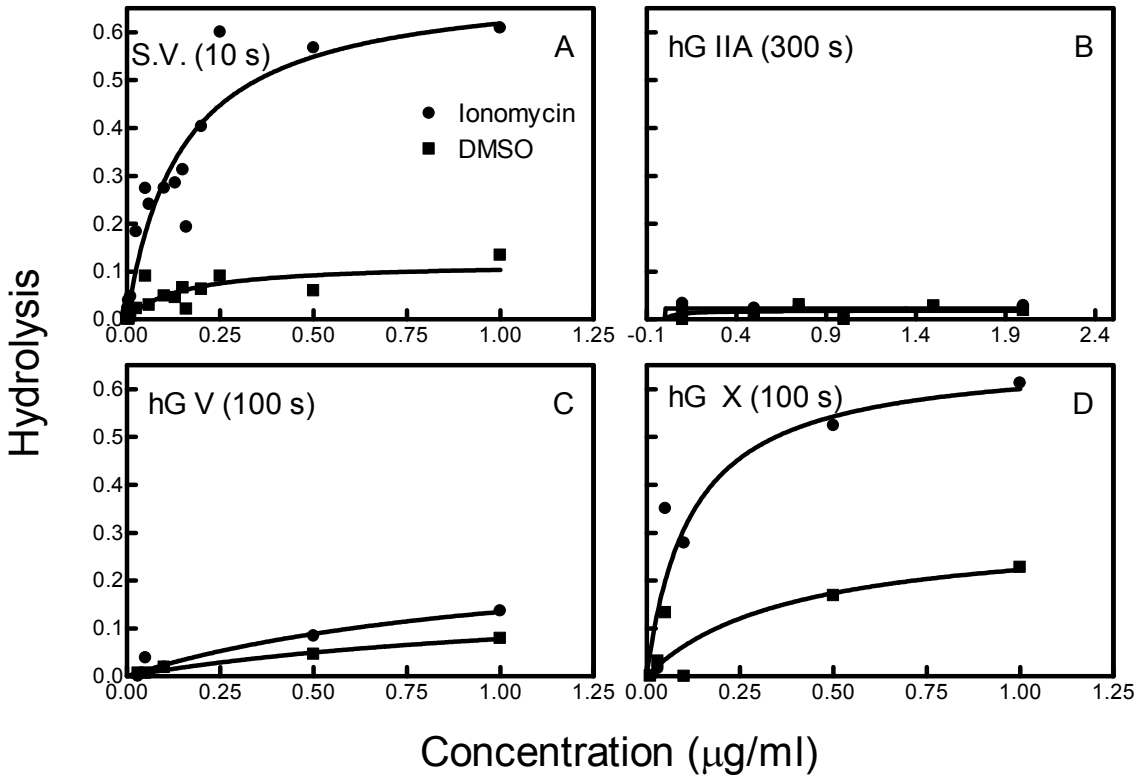
S.V. (10 s)
A
Ionomycin
DMSO
hG IIA (300 s)
B
hG V (100 s)
C
hG X (100 s)
D
Hydrolysis
Concentration (μg/ml)

FIGURE 6

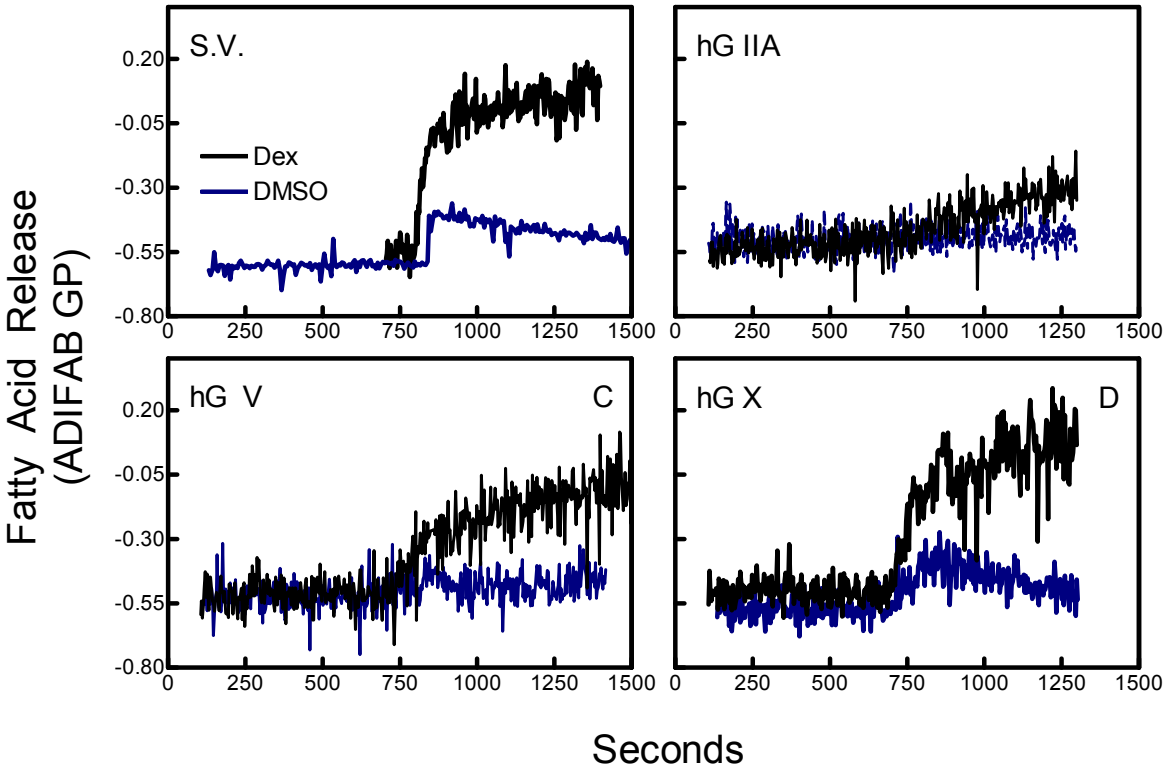
S.V.
hG IIA
hG V
C
hG X
D
Dex
DMSO
Fatty Acid Release
(ADIFAB GP)
Seconds
0.20
-0.05
-0.30
-0.55
-0.80
0
250
500
750
1000
1250
1500

FIGURE 7

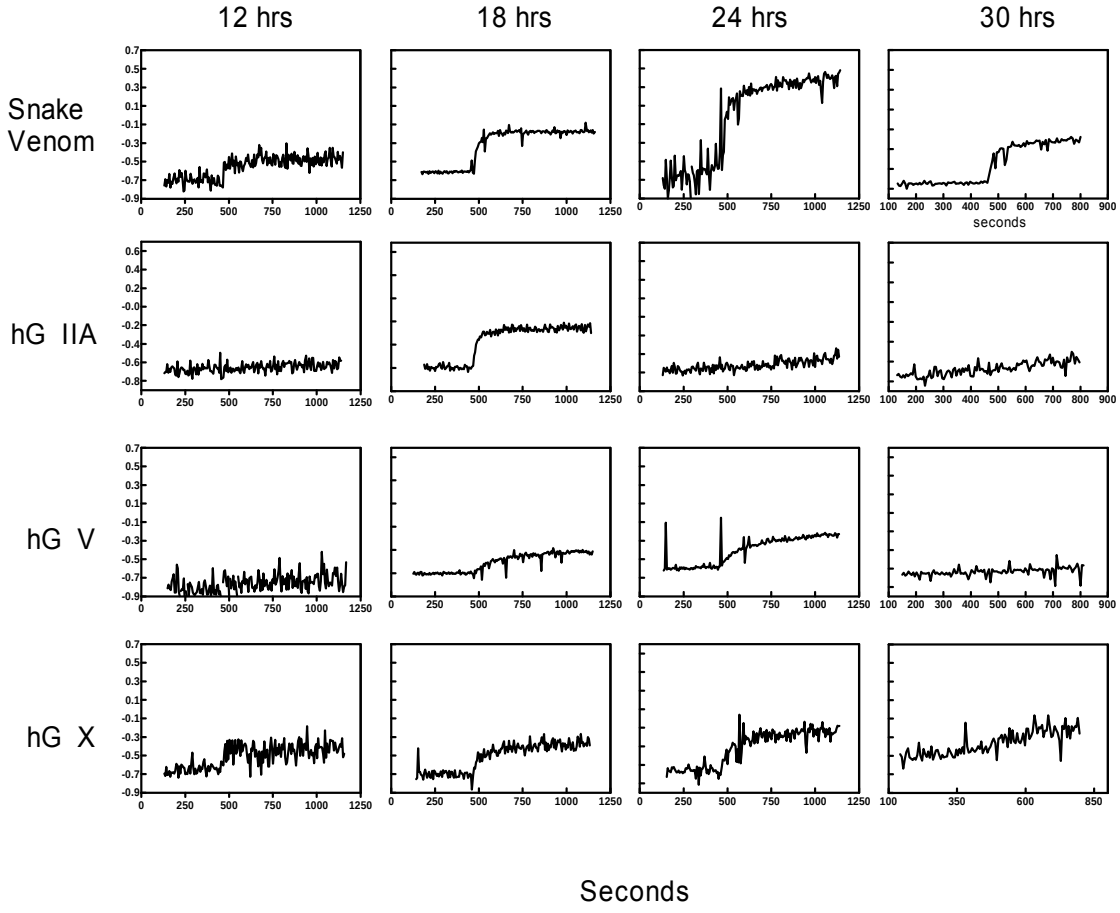
12 hrs
18 hrs
24 hrs
30 hrs
Snake Venom
hG IIA
hG V
hG X
seconds
Seconds

FIGURE 8

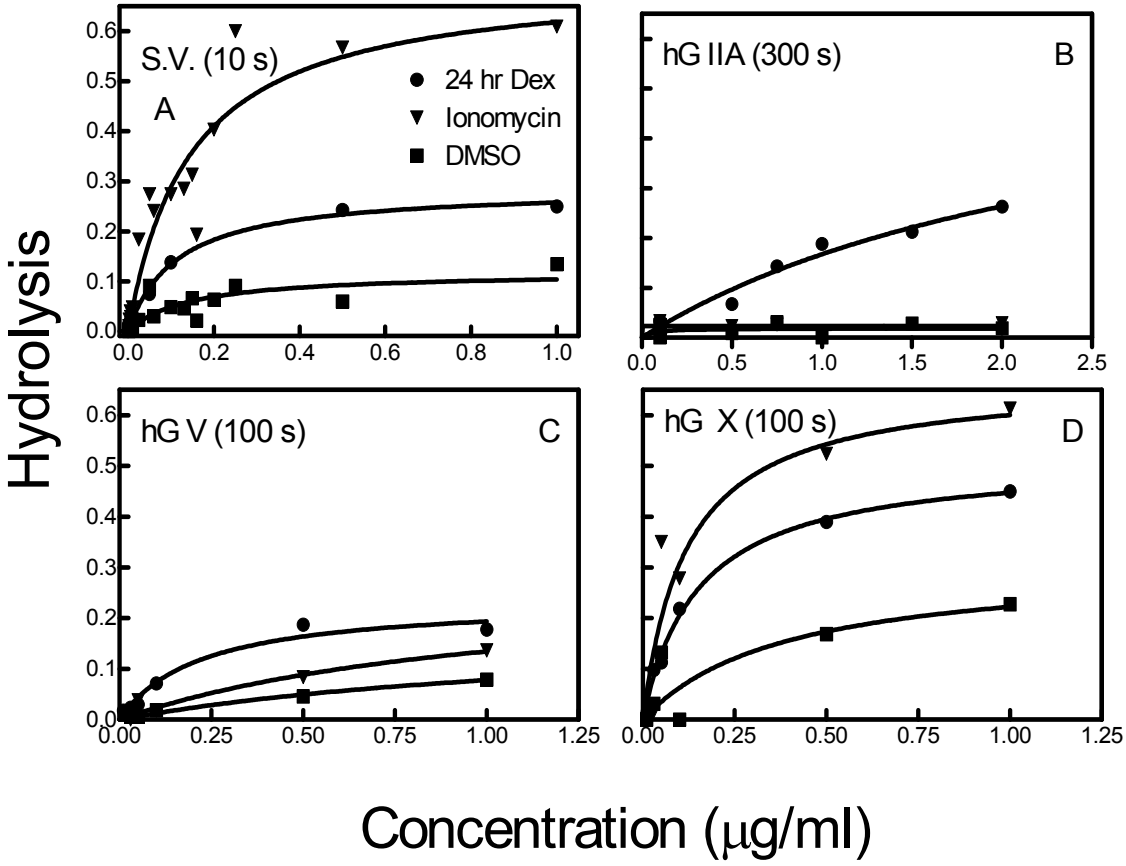

Enzyme	DMSO	Ionomycin	Dexamethasone
Snake Venom	0.1446	0.1456	0.1135
hG IIa	N/A	N/A	2.715
hG V	1.325	1.082	0.2204
hG X	0.3888	0.1187	0.1503

FIGURE 9

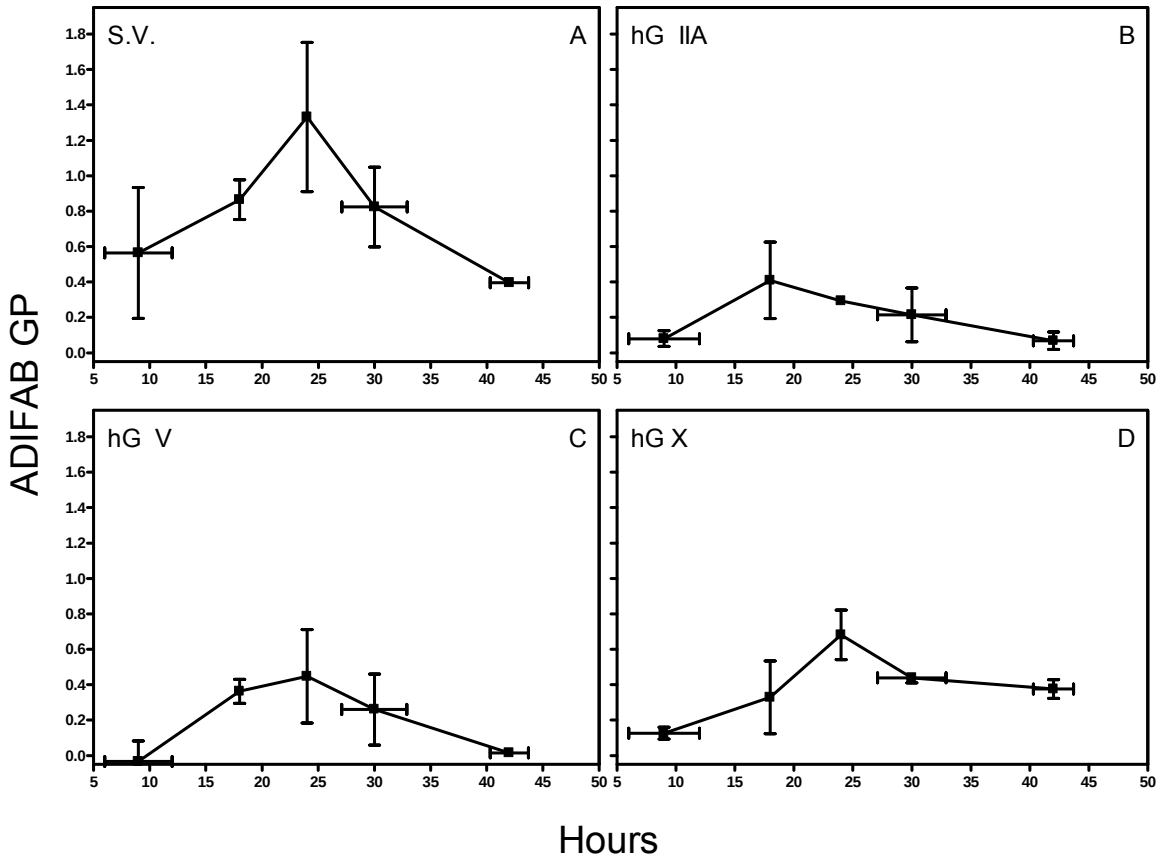

FIGURE 10

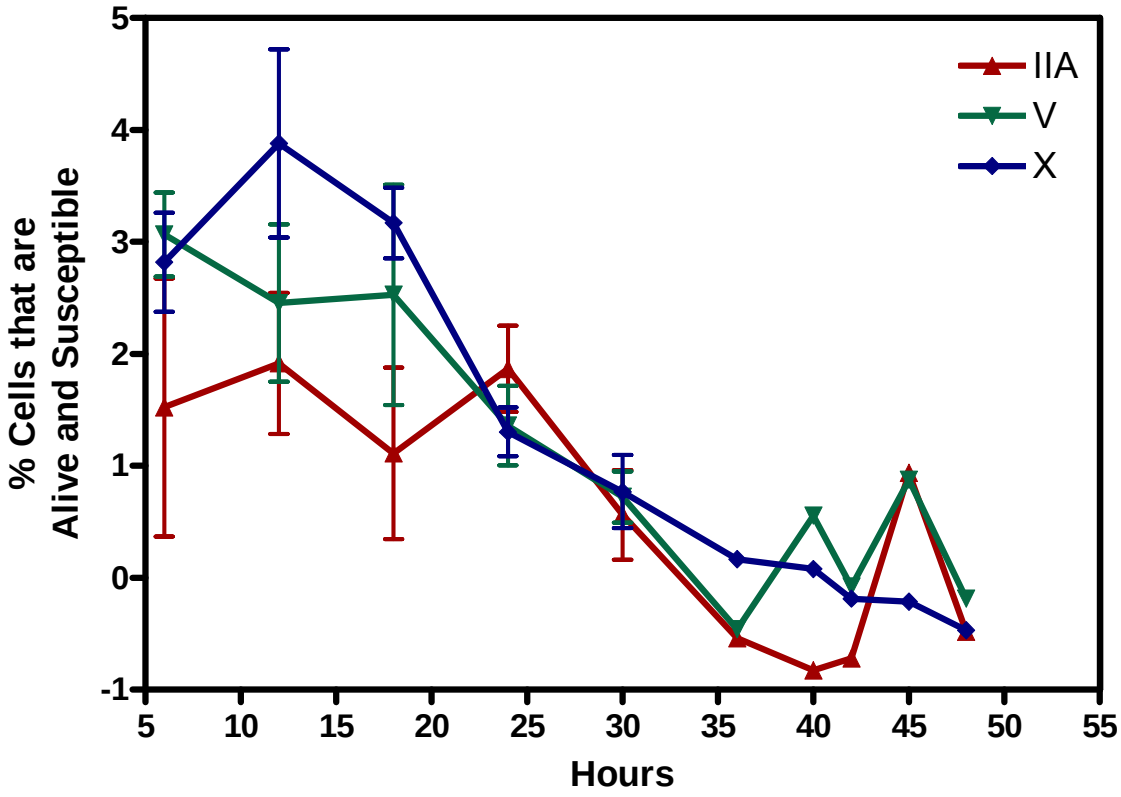
% Cells that are Alive and Susceptible
Hours
IIA
V
X
5
4
3
2
1
0
-1
5
10
15
20
25
30
35
40
45
50
55

FIGURE 11

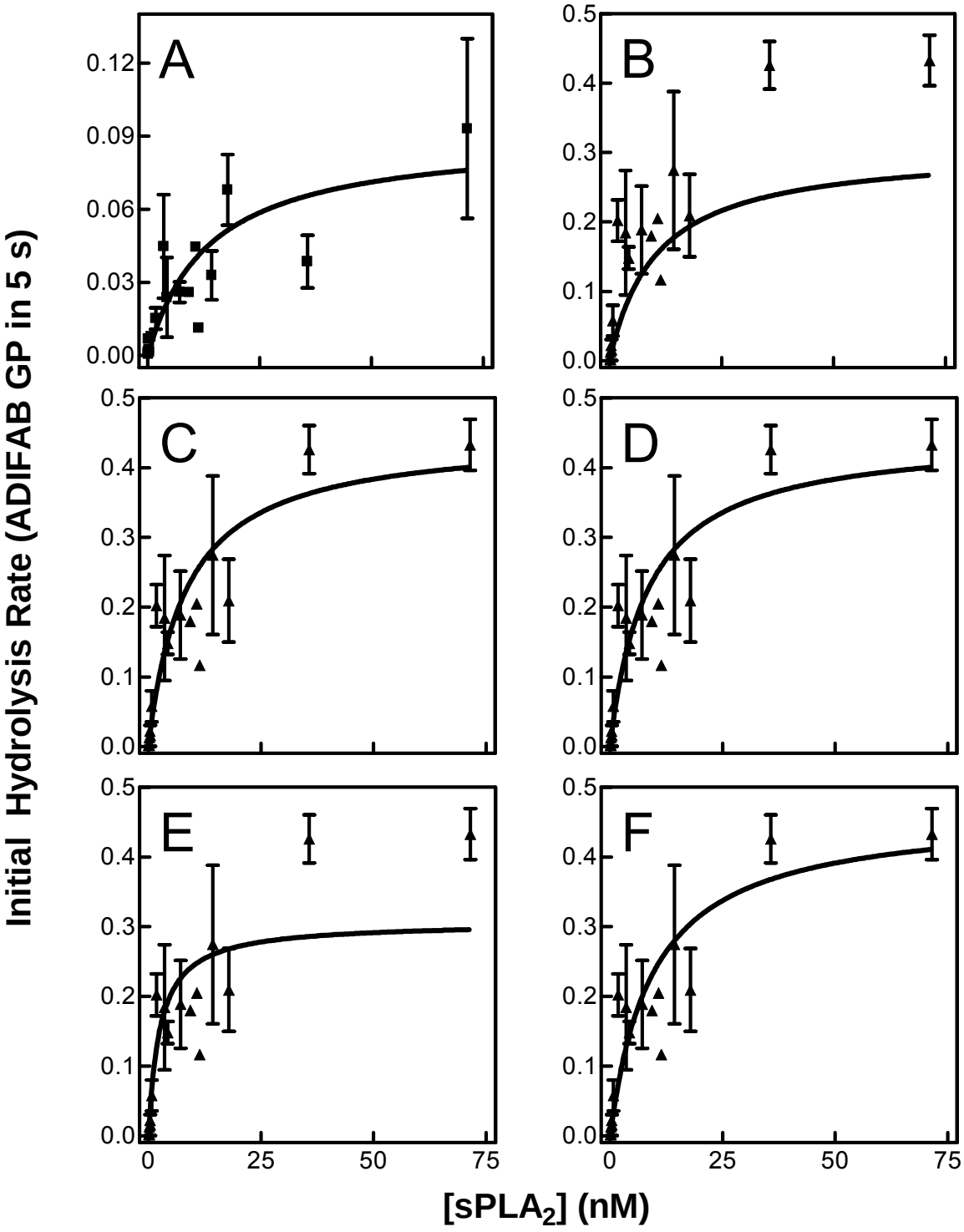
A
B
C
D
E
F
Initial Hydrolysis Rate (ADIFAB GP in 5 s)
[sPLA2] (nM)
0.00
0.03
0.06
0.09
0.12
0.0
0.1
0.2
0.3
0.4
0.5
0
25
50
75

FIGURE 12

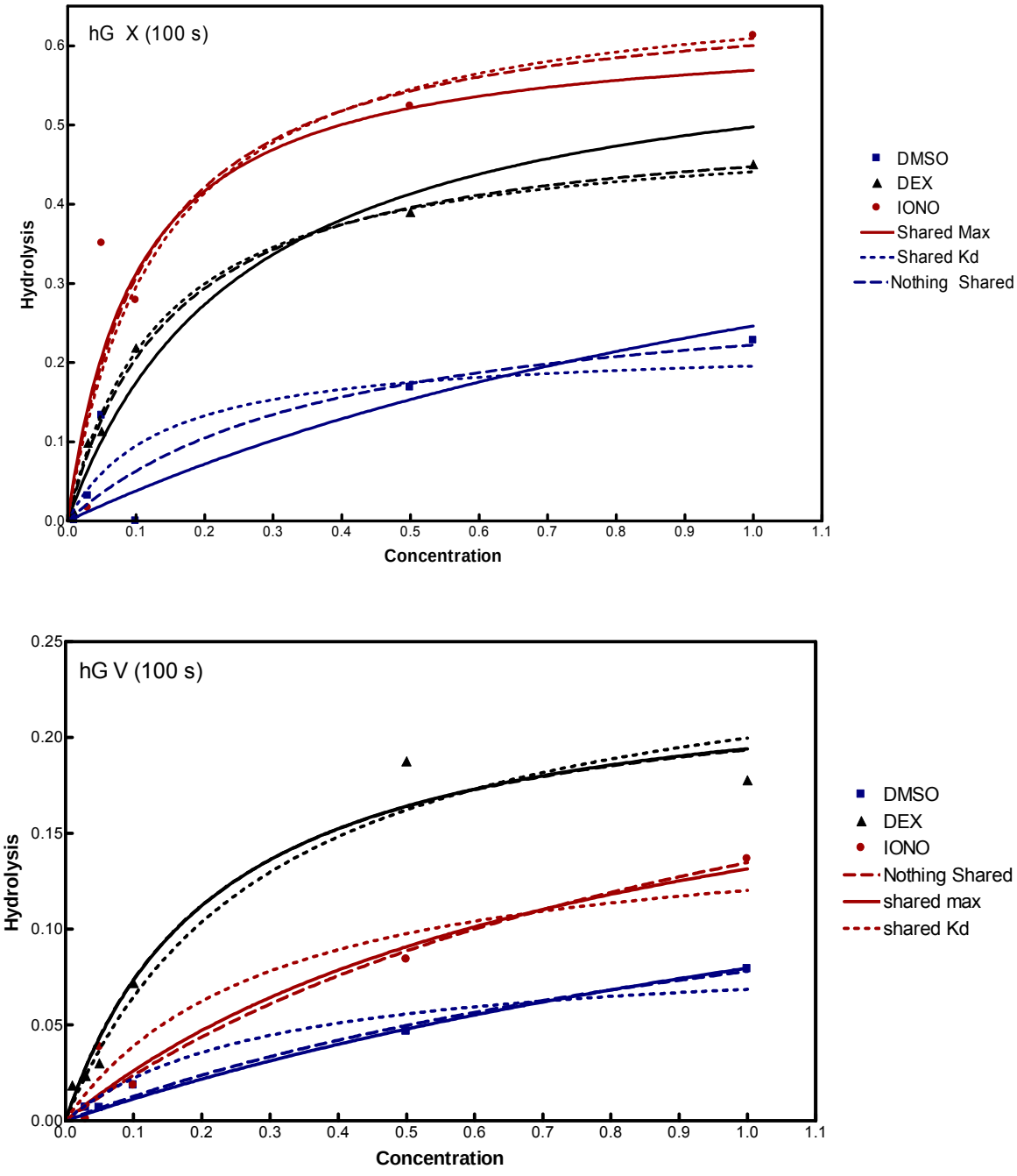
hG X (100 s)
Hydrolysis
Concentration
0.0
0.1
0.2
0.3
0.4
0.5
0.6
0.7
0.8
0.9
1.0
1.1
DMSO
DEX
IONO
Shared Max
Shared Kd
Nothing Shared
hG V (100 s)
Hydrolysis
Concentration
0.00
0.05
0.10
0.15
0.20
0.25
DMSO
DEX
IONO
Nothing Shared
shared max
shared Kd

Erin D. Olson
1730 Spring Oaks Dr
Springville, Ut 84663
1-702-239-1367
Diedre_Dalene@hotmail.com

Education

Brigham Young University, Provo, UT
Masters in Physiology and Developmental Biology **2006-2008**
Thesis: "Analysis of Hydrolysis Kinetics by sPLA2 Isoforms During Apoptosis in S49 Cells." Thesis defended on June 30, 2008

Brigham Young University, Provo, UT
B.S. in Biology **2002-2006**
Areas of Concentration: Human Physiology, Biophysics
Minor: Geology

Brigham Young University, Rexburg, ID
Associates Degree **2001-2002**
Areas of Concentration: Physical Sciences

Work & Teaching Experience

Brigham Young University, Graduate Studies
Department Representative – Graduate Student Society **2007-2008**
Help organize monthly student events; acted as an ambassador between the university and the graduate students.

Brigham Young University, Physiology Developmental Biology
Research Assistant – Bell Lab **2004-2008**
Designs and Conducts spectroscopy and microscopy experiments; performs statistical analysis of data using Microsoft Excel or Prism Graphpad software; maintains lymphoma cell cultures; presents research at weekly lab meetings and weekly departmental journal club; trains multiple new assistants each year; organizes and coordinates schedule of laboratory resources.

2006-2007
Teaching Assistant - Physiology Lab
Administered weekly quizzes and laboratory assignments for 100 students; taught weekly two-hour laboratory sessions; met individually with students 3-4 hours weekly.

Brigham Young University – Idaho, Geology
Teaching Assistant **– for Dr. Edmund Williams, "Introduction into Geology"** **2002**
Organized daily trips into the field to study geology; administered weekly quizzes and laboratory assignments for 10 students; taught weekly laboratory sessions; met individually with students weekly.

Brigham Young University – Idaho, Geology

Teaching Assistant – **for Dr. Edmund Williams, "Field Geology"** **2002**
Administered weekly quizzes and assignments for 30 students; planned and taught weekly one-hour sessions; met individually with students 3-4 hours weekly.

Publications

Published:

- Jensen, L.B., Burgess, N.K., Gonda, D.D., Spencer, E., Wilson-Ashworth, H.A., Driscoll, E., Vu, M.P., Fairbourn, J.L., Judd, A.M., and Bell, J.D. (2005) *Mechanisms Governing the Level of Susceptibility of Erythrocyte Membranes to Secretory Phospholipase A_2*. Biophys. J. 88: 2692-2705.

- Bailey, R.M., Olson, E.D., Vu, M.P., Brueseke, T.J., Robertson, L., Parker, K.H., Judd, A.M., and Bell, J.D. (2007) *Application of Membrane Biophysics to Cell Physiology: Mechanisms by which Apoptotic Membranes Become Susceptible to Secretory Phospholipase A2*. Biophys. J. 93: 2350-2362.

In Progress:

- Olson, ED; Nyugen, T; Bailey, R W; Gibbons, E; Judd, A; Bell, J D. *A Comparative Analysis of Hydrolysis Kinetics of sPLA2 Isoforms*

- Bailey RW, Olson ED; Gibbons E; Nguyen T; Robertson L; Judd AM; Bell JD. *Determinants of App D49 secretory phospholipase A2 activity in S49 cells during glucocorticoid-induced apoptosis*

Oral Presentations & Research Abstracts

- Olson, ED; Nyugen, T; Bailey, R W; Gibbons, E; Judd, A; Bell, J D. *A Comparative Analysis of Hydrolysis Kinetics of sPLA2 Isoforms.* Biophysical Society 52nd Annual Meeting & 16th International Biophysics Congress. February 6, 2008.

- Olson, ED; Nyugen, T; Judd, A; Bell, J D. *An Analysis of Hydrolysis Kinetics of $sPLA_2$ Isoforms Dexamethasone Induced Apoptosis.* Cancer Research Center Fellowship Presentations. Summer Cancer Workshop. August 15, 2007.

- Bailey RW, Olson ED; Vu MP; Brueseke TJ; Robertson L; Parker KH; Judd AM; Bell JD. *Application of Membrane Biophysics to Cell Physiology: Mechanisms by which Apoptotic Membranes Become Susceptible to Secretory Phospholipase A2*. Biophysical Society 51st Annual Meeting & 15th International Biophysics Congress. March 7, 2007.

- Olson ED. *Defense of Prospectus of Research for Master's Thesis.* Presented to Thesis Committee: Dr.s John Bell, Allan Judd, & Allen Buskirk. November 20, 2006.

Professional Memberships

- Biophysical Society
  2006-2008

Fellowships, Grants & Scholarships

- *A Comparative analysis of Hydrolysis Kinetics of sPLA$_2$ Isoforms in s49 Lymphoma Cells*. Research under the direction of Dr. John Bell. Funded through the BYU Cancer Research Center. April/August 2007. Funded for $6,775.

- *Application of Membrane Biophysics to Cell Physiology: Mechanisms by which Apoptotic Membranes Become Susceptible to Secretory Phospholipase A$_2$.* Undergraduate research under the direction of Dr. John Bell. Funded through the BYU Office of Research & Creative Activities. April 2006. Funded for $1,500.
- Half-tuition Undergraduate Scholarship. Brigham Young University. 2002-2003
- Half-tuition Undergraduate Scholarship. Brigham Young University-Idaho. 2001-2002
- Target Students in Excellence Scholarship. Target. 2001.

Community Service & Leadership

Church of Jesus Christ of Latter Day Saints
Religious Volunteer – Springville area **2007-2008**
Help organize monthly events for religious activities; provided assistance to other members of the congregation when in need.

Brigham Young University, Center for Service and Learning
Volunteer Tutor – Biology and Physiology **2002-2007**
Conducted weekly meetings with 1-3 undergraduates per semester; taught proper study habits, note-taking and organization skills.

St. Rose Dominican Hospital
Emergency Room Volunteer**– for Dr. Rick Henderson** **2002-2005**
Help check patients into emergency care treatment; provided comfort for family members in need; assisted doctors when needed.

Skills & Certifications

- Proficient in Excel, Prism Graphpad graphing and statistical software, PowerPoint, and QUICK BASIC
- College Reading and Learning Association, certified level 1 tutor.